



**UNIVERSIDAD DE INVESTIGACIÓN DE
TECNOLOGÍA EXPERIMENTAL YACHAY**

Escuela de Ciencias de la Tierra, Energía y Ambiente

**TÍTULO: Incidence of Physical Weathering by Salt Growing
Deterioration Process Associated to the Aggregates Employed in
the Architectural Structures of the Riobamba City**

Trabajo de integración curricular presentado como requisito para la
obtención del título de Geólogo.

Autor:

Hernandez Jhónnatan

Tutores:

Ph.D Vázquez Yaniel

Ph.D Ávila Edward

Urcuquí, mayo 2024

AUTORÍA

Yo, **HERNANDEZ MENDOZA JHÓNNATAN ANDRÉS**, con cédula de identidad 0604418475, declaro que las ideas, juicios, valoraciones, interpretaciones, consultas bibliográficas, definiciones y conceptualizaciones expuestas en el presente trabajo; así como, los procedimientos y herramientas utilizadas en la investigación, son de absoluta responsabilidad del autor del trabajo de integración curricular. Así mismo, me acojo a los reglamentos internos de la Universidad de Investigación de Tecnología Experimental Yachay.

Urcuquí, mayo de 2024.

Jhónnatan Andrés Hernandez Mendoza

CI: 0604418475

AUTORIZACIÓN DE PUBLICACIÓN

Yo, **HERNANDEZ MENDOZA JHÓNNATAN ANDRÉS**, con cédula de identidad 0604418475, cedo a la Universidad de Investigación de Tecnología Experimental Yachay, los derechos de publicación de la presente obra, sin que deba haber un reconocimiento económico por este concepto. Declaro además que el texto del presente trabajo de titulación no podrá ser cedido a ninguna empresa editorial para su publicación u otros fines, sin contar previamente con la autorización escrita de la Universidad.

Asimismo, autorizo a la Universidad que realice la digitalización y publicación de este trabajo de integración curricular en el repositorio virtual, de conformidad a lo dispuesto en el Art. 144 de la Ley Orgánica de Educación Superior

Urcuquí, mayo de 2024.

Jhónnatan Andrés Hernandez Mendoza

CI: 0604418475

Agradecimiento

Quiero expresar mi más profundo agradecimiento a las personas que han sido fundamentales en mi vida. En primer lugar, a mi madre, quien con un esfuerzo incansable y una paciencia inagotable siempre estuvo a mi lado durante mi tiempo en la universidad, brindándome un apoyo incondicional a pesar de mis errores y desaciertos.

Agradezco también a mi Tía Luz Angelita Mendoza, cariñosamente conocida como Luchita, quien ha sido un pilar fundamental en mi vida, compartiendo tanto mis logros como mis fallos, y siempre ofreciéndome su amor y cariño.

Mi reconocimiento también se extiende a mi padre, quien, de diversas maneras, ha intentado formar parte de mi vida a pesar de nuestras diferencias. A mi hermano, que ha sabido salir a delante por sus propios méritos y me ha motivado a superarme cada día.

No puedo dejar de mencionar a mis tíos German Criollo y Blanca Mendoza, quienes siempre han estado a mi lado, brindándome su apoyo a lo largo de los años, especialmente en los momentos más difíciles, gracias a los cuales he logrado salir adelante.

Agradezco a mis primos Gaby, Mishel, Israel, Ángelo, Jairo, Víctor, Pablo C., Maira, Vero, Pablo M. y Adriana, quienes han sido compañeros de vida, de quienes he aprendido mucho viéndolos crecer como personas excepcionales. Ellos me han enseñado que los problemas pueden resolverse y que siempre podemos contar los unos con los otros, recordándome que nunca estamos solos.

Por último, deseo expresar mi más sincero agradecimiento a mis tutores en este proyecto, el Dr. Yaniel Vázquez y el Dr. Edward Ávila. Su inestimable apoyo, dedicación y paciencia fueron elementos cruciales para llevar este proyecto a buen término.

Jhónnatan Andrés Hernandez Mendoza

Resumen

Riobamba conocida como “La ciudad bonita” es una de las ciudades emblemáticas del Ecuador, siendo un atractivo turístico tanto para visitantes nacionales como para extranjeros; sin embargo, el deterioro de las obras civiles por la acción de sales (haloclastia), puede poner en peligro el atractivo de la ciudad. Recorriendo las principales calles de la ciudad es fácil constatar que la formación de sales en las fachadas de las edificaciones es un problema recurrente. Pese a esto, no se ha realizado ningún estudio que determine cuales son las principales fases minerales responsables del deterioro de las obras civiles además de cuál y como es el grado de afectación de estas.

Este trabajo tiene como objetivo mostrar el nivel de incidencia de la meteorización física causada por el proceso de formación de sales en las obras arquitectónicas de la ciudad de Riobamba y su relación con los diferentes agregados empleados en cada uno de los morteros y concretos necesarios para cada una de las estructuras.

Para lo cual primero fue necesario establecer el grado actual de deterioro de las obras arquitectónicas, además de la procedencia de los materiales que se usan en la construcción de las mismas. Posteriormente se realizó un muestreo de las sales responsables del deterioro. Finalmente, las fases minerales fueron determinadas empleando el análisis por difracción de rayos X (DRX). El análisis de treinta y dos muestras, recolectadas en el sector conocido como El Retamal, permitió establecer que las principales fases minerales responsables del deterioro de la obra civil en la ciudad de Riobamba corresponden a: thenardita, calcitas y nitratina.

Palabras clave: sales, meteorización, morteros, eflorescencia, erosión.

Abstract

Riobamba known as "La ciudad bonita" is one of the emblematic cities of Ecuador, being a tourist attraction for both national and foreign visitors; however, the deterioration of civil works due to the action of salts (haloclasty), can endanger the attractiveness of the city. Walking through the main streets of the city it is easy to see that the formation of salts on the facades of buildings is a recurring problem. Despite this, no study has been carried out to determine which are the main mineral phases responsible for the deterioration of civil works, as well as which and how they are affected.

This work aims to show the level of incidence of physical weathering caused by the salt formation process in the architectural works of the city of Riobamba and its relationship with the different aggregates used in each of the mortars and concretes necessary for each one of the structures.

For this goal, it was first necessary to establish the current degree of deterioration of the architectural works, in addition to the origin of the materials used in their construction. Subsequently, a sampling of the salts responsible for the deterioration was carried out. Finally, the mineral phases were determined using X-ray diffraction analysis (XRD). The analysis of thirty-two samples, collected in the sector known as El Retamal, allowed us to establish that the main mineral phases responsible for the deterioration of civil works in the city of Riobamba correspond to: thenardite, calcite and nitratine.

Keywords: salt, weathering, mortar, efflorescence, erosion.

Index

Resumen.....	i
Abstract	ii
1 Introduction	13
2 Objectives	16
2.1 General Objective	16
2.2 Main Objectives	16
3 Theoretical framework	16
3.1 Weathering.....	16
3.1.1 Chemical Weathering.....	17
3.1.2 Mechanical or Physical Weathering.....	18
3.1.3 Mechanical Behavior.....	18
3.1.3.1 External Stress	19
3.1.3.2 Internal Stress	20
3.1.4 Haloclasty.....	20
3.1.5 Mechanisms of Salt Damage.....	21
3.2 Salt Damage in Architectural structures	21
4 Geology and Weather Framework.....	23
4.1 Regional geology	23
4.1.1 Inter Andean Depression.....	23

4.2	Local Geology.....	25
4.2.1	Lithological Units.....	25
4.3	Weather of the Region	27
5	Architectural structures in Riobamba City	30
6	Methodology and Materials.....	32
6.1	Building materials and their provenance.	32
	Bricks	32
	Iron rods:	33
	Cement:	33
	Aggregates (Sand and Stones):	34
	Water:.....	35
6.2	Sampling	36
6.3	X-ray Diffraction Analysis	37
	X-Ray Diffraction Analysis (XR-D):.....	39
	Data Processing.....	40
7	Results	42
7.1	Deterioration of Architectural structures	42
	Characterization of the Deterioration Process.....	45
7.2	Building Materials Analyses.....	46
	Quarries	47
	Geology of the Quarries	47

Way of Mining and Aggregates Expended	51
Chemical Analysis of the R-DAD and the Aggregates.....	56
7.3 Mineral Phases Responsible of the Deterioration of Architectural structures	58
Sulfates:.....	63
Carbonates:.....	63
Nitrates:	64
8 Discussion.....	66
9 Conclusion and Recommendation	69
9.1 Conclusion	69
9.2 Recommendations.....	72
10 References.....	73
11 Annexes.....	79

Figure Index

Figure 1. Ecuadorian Tectono-Stratigraphic Regions. The figure shows the six tectono-stratigraphic regions, that conform Ecuador. From oldest to youngest these correspond to: Amazon Basin, Sub-Andean Zone, Eastern Cordillera, Inter-Andean Depression (AID), Western Cordillera, and Coastal Plain (Winkler et al., 2005). Riobamba city, the capital of Chimborazo province, is located in the south of the AID at 211 km, through the highway Panamericana-E35, with respect to Quito City (capital of Ecuador). The Chimborazo volcano is placed in the Western cordillera and represents one of the most important tourist attractions of Riobamba Ecuador. 15

Figure 2. Geological Map of Riobamba City. This map shows the special distribution of the different geological units presents in the city. The Riobamba Unit R-DAD is the predominant and emerges the north and east of the city, the rest emerges at the south-west. The red and orange rectangles show the areas designed for mining y the municipality of Riobamba through the time. From these, red rectangles show the zones that still working. The map also shows the specific location of each quarry visited by the development of this project IGM (2012). 28

Figure 3. Historical Heritage Buildings of Riobamba city. La Catedral church, Edificio del Correo, Municipio de la ciudad de Riobamba and La Basilica church. Architectural structures of Gothic stile. 30

Figure 4. Republican Buildings in Riobamba city. The figure shows the typical republican buildings and its classification according to the ending of the building. a) shows a typical republican building built in base of concrete, bricks, iron, and aggregates. Likewise, a) is a white work building because the walls are cover by a white plaster and painted b) this picture shows a building where the ground floor corresponds a white work. However, the upper floors are designed as gray work building due to, the endings correspond a wall cover by mortar without protection against the environment. Finally, both walls showed in c) there are two different black work building because bricks (terracotta, concrete) and columns does not have any protection (mortar, paint) against the environment (Author). 31

Figure 5. Terracotta and Concrete Bricks. a) shows the form of terracotta bricks employed to build the different infrastructure in Riobamba city. b) shows the form how concrete brick is exposed to be expended (Gavilanes & Santellan, 2016).33

Figure 6. Iron Rods. Iron rods structures employed to enforce slabs and columns. These structures are directly cover by concrete (Adelca, 2020).33

Figure 7. Holcim and Chimborazo Cement. The figure shows the typical presentation of the 50kg bag of Hydraulic Cement Type GU from the most important companies Holcim and Cemento Chimborazo. According with the normative of construction of Ecuador the GU type cement most be employed in general for buildings that does not need special specifications.....34

Figure 8. Mira Flores Quarry. The figure shows a typical quarry in Riobamba city. This quarry corresponds to Mira Flores and it is located at the north of the city in the Panamericana E-35 highway. In the background of the image, it is possible to see how heavy machinery mined the material from the deposit. This material posteriorly is sifted to be expended at the citizens (Author).....35

Figure 9. Study Zone. The map shows the northwest part of Riobamba city known as El Retamal. The red triangles show the points where the different samples were taken. The principal streets and avenues travelled corresponds to: Av. Sergio Qirola, Av. 11 de Noviembre and, Oswaldo Guayasamin, Eduardo Kingsman, Segundo Rosero Alfredo Gallegos streets (Author).....37

Figure 10. Sample processing: The pictures show the different steps necessities to the samples turns adequate for the XRD analysis. The picture (a) shows the pulverization of the sample, while (b) shows the correct way to emplaces the samples in the molds (Author).39

Figure 11. XR-D analyzer from the Yachay Tech university. The samples are scanning in the machine located at the right. Posteriorly, the data is digitalized and saved in the computer located to the left (Author).....40

Figure 12. Interference Figure. The blue line represents the interference figure obtained as data from the XRD analyzer. This figure is processed by the software Match! To identify the different mineral phases present in the sample (Author).41

Figure 13. Historical Heritage Buildings of Riobamba City. The figure shows three different kind of historical heritage buildings which were covered or fixed by modern mortar. In these three buildings the salt growing process is limited to the zones covered by modern mortars. The picture a) shows a big hole where the mortar has been removed exposing the rammed earth, inside the wall, to the environment. In the picture b) the deterioration is associated at the mortar surrounding the volcanic rocks arranged in the base of the wall. Finally, picture c) shows slat growing affectation in the façade of the building (Author).43

Figure 14. Several Cases of Salt Growing. The figure shows a several cases of slat growing where the mortar that cover the walls and the concrete that covers the iron rods have been removed. Likewise, the iron rods exposed in the lower part of the column show signs of oxidation. Even though the iron rods are exposed, no flexion of the concrete column is seen (Author).....44

Figure 15. Salt Growing Incidence in Republican Buildings. The left figure shows the relationship between the salt growing phenomenon with the different mortars and bricks employed in civil architecture. The right figure shows the incidence of salt growing according the three kinds of republitan building (Author).45

Figure 16.. Distribution of the Problematic around the Riobamba city. This figure represents six different republican buildings located in different parts of the city where the salt growing deterioration is present especially in façades, but it is also inside the buildings. The pictures A, B, C, and the ground floor of picture E represent white work buildings affected by salt growing producing the deterioration of the facades. Picture D shows how salt growing process affects gray work buildings. Finally, F shows that salt growing also occurs in the internal walls of the buildings (Author).....46

Figure 17. Spatial Distribution of the Facies that Conforms the R-DAD. This corresponds mined slope from the Sillahuan quarry locates at the west of the city. The deposit reaches up 50 m. This is composed of two facies, the Mf (2) in the bottom with the Bf (1) over this. The Mf shows light colors corresponding a matrix supported massive deposit. On the other hand, the Bf show more dark colors, although this is a matrix supported deposit too, here it is possible to appreciate clasts of different size (Author).....48

Figure 18. Mixed Facies Mf. The Mf shown in the figure belongs to a mined slope from the Mira Flores quarry located in the north of the city. Here the Mf reaches up 22 m. Inside this

deposit is contained diaclased rocks of around 1.5 m in size (1). Likewise, it is possible to distinguish some intrusions that correspond to yellow pipes. These pipes reach up to 3 m of thickens (2) (Author).....49

Figure 19. Block Facies Bf. The Bf shown in the figure belongs to a mined slope from the Cerro Negro quarry located in the east of the city. Here the Mf reaches up to 22 m. this consist of a matrix-supported massive deposit poorly sorted. The clast size varies from 3 to 45 cm (Author).....50

Figure 20. Cerro Negro Quarry. This corresponds to one of the oldest quarries in the city. The figure is composed of three pictures that shown the mining process. image (a) shows a typical quarry in the city where the material is mined employing heavy machinery forming terraces. e image (b) shows a sieve employed to separate the sand and stones from the material mined. image (c) shows a shredded employed to reduce big clasts into smaller rocks known as ripio (Author).....52

Figure 21. Fine Sand for Plastering mortars. The fine sand marketed independently of the quarry comes from a sifting process. Fine sand is composed of 90% fine sand and a 10% of lithics. The different pictures show the same sand under different levels of zoom amplification (Author).53

Figure 22. Medium to Coarse Sand. This kind of sand is employed for mortars to join bricks. This sand is composed of 80% medium sand grain size and 20% of lithics. This kind of sand comes in two different ways. The first corresponds to a sifting process and the second is a shredded process. The figure shows shredded sand, taken from Mira Flores quarry, under different levels of zoom amplification (Author).....54

Figure 23. Ripio. Is known as Ripio at the mixture of rocks composed of: andesites, amphibole andesites, amphibole-pyroxene andesites, amphibole-plagioclase andesites and, tuffs, expended as aggregate by the concrete to produce concrete, employed in slabs and columns. To be considered as Ripio the size of rocks must be between 10 to 51 mm (Author).55

Figure 24. Percentage Distribution of the Different Mineral Phases Responsible in the Deterioration Process. This figure is composed of two graphics that represents the percentage distribution of the different mineral phases and salts responsible for the deterioration process

in architectural structures of Riobamba city. The part a) represents the mineral phases and the part b) the salts species. Both graphs summarized the data exposed in Table 6, where the results from XRD are shown (Author).....58

Table Index

Table 1. Specific location of the 32 samples selected by the XR-D analysis. The table also shows the structure where the sample was taken.	38
Table 2. Kind of Aggregates marketed in each one of the quarries visited by the author.	51
Table 3. Chemical composition of samples associated with R-DAD taken from the works of Barba (2016) and Clapperton (1990).	56
Table 4. Chemical composition of the sieved sand sold as fine sand from the Cerro Negro quarry. Fine sand mixed with water and cement form the mortars that will be employed in the endings of the building (facades, and to cover walls columns, and roofs).	57
Table 5. Chemical composition of the shredded sand sold as medium to coarse sand from the Cerro Negro quarry. Medium to coarse sand mixed with water and cement form the mortars employed to join bricks to build walls. In addition, Medium to coarse sand mixed with water, ripio and cement produce concrete.	57
Table 6. XRD results: The table shows the different phase minerals responsible for the deterioration process of the architectural structures in Riobamba city. To obtain these minerals was necessary to apply XRD analysis over these samples. This table, in addition to the mineral phases, also shows the formula, the crystal system, and the percentage of the mineral respect to the whole sample.	59

Annexes Index

Annex 1. Table of chemical characteristics of water from the different wells that supplies to Riobamba city.....	79
Annex 2. Table of aggregates expended in each quarry active in Riobamba city.	79
Annex 3. Table of hand sample description of the different rocks that constitute the Ripio expended in the different quarries in Riobamba city.	80
Annex 4. Table of samples taken in EL Retamal. The table indicates the specific location of each sample from where was taken, likewise, specifies the kind of building and the walling material where the salt is affecting.	84

1 Introduction

In the last decades the interest in the decay process of building materials has increased, especially in the attempts to understand the deterioration process caused by salt growing weathering, also known as haloclasty (Haynes, 2002). Weathering is a natural process that occurs throughout our planet from the coldest to the warmest zones. This process consists of the physical and chemical change of the ground through the time, due to the action of atmosphere, hydrosphere, cryosphere, biosphere, and nuclear radiation (Hack, 2020). Around the world, weathering is widely recognized as the major agent in the deterioration process of historic and archeological structures, due to the action of this over the ground-matter employed in those structures (Doehne, 2002; Hack, 2020). One of the most common ways this occurs consist in form of deterioration by salt attack or salt growing. Salt growing usually occurs when sulfate is present however, not only sulfates are responsible for weathering, sodium carbonates, and sodium chloride have the same impact (Haynes, 2002).

The deterioration process associated with salt growing is a common problem around the world. In the American continent, several studies have been carried out on this problem. Haynes in (2002) presents a review about this problem in the United States of America. This review covers from 1968 until 2002. In his work found that the major of cases that present salt growing corresponds to structures built with ordinary Portland cement or extremely poor-quality concrete. The mortars and concretes built with these kinds of cements showed a lost in mass and strength, however, this phenomenon did not represent a real structural problem.

In the same way, this phenomenon has been studied in South America. Among the most important are the studies carried out in Chile and Brazil. These studies indicates that the deterioration of architectural structures associated to salt attack is a common problem in the region (Tapia, 2015). It is important to mention that both studies point to sulfates as the main salts responsible for this phenomenon.

In Ecuador. the deterioration of infrastructures as the result of physical weathering produced by salt growing (haloclasty) is a common problem. It is present in the three natural regions Coast, Andean. and Amazonian.

Riobamba, the capital city of the Chimborazo province, is located in the Andean region. This city is in the geographic center of Ecuador at 211 km from Quito (the capital of Ecuador)

through the Panamericana E35 (Figure 1). In Riobamba city the deterioration of architectural structures associated with salt growing is a common and evident problem.

The deteriorations associated to salt growing represents a continuous economic problem for the citizens. The owners, seeing the facades of the different buildings affected, must invest in maintenance to prevent the devaluation in the cost of marketing. In many conversations taken with the owners of the different architectural structures, they indicate that the cost of reparation is high. However, there are no official data about the economic cost that this problem represents. In addition, this phenomenon represents an aesthetic problem not only by the owners, but also for the city itself. Because, Riobamba city is considered as a tourist destination for foreigners.

Riobamba City corresponds a valley surrounded by a mountainous landscape. From this city is possible to see different volcanoes such as: El Altar, Tunguragua, Carihuairazo and Chimborazo. The Chimborazo volcano (6 263masl) located in the south of the Western Cordillera (Figure 1), also known as the closest point to the sun, is one of the most important touristic destinations in Ecuador (EL Comercio, 2016). This volcano is visited by national and foreign tourists. The tourist uses Riobamba City as a place to stay and adapt the body at high altitudes (2 754masl) previously to visit the volcano. During their stay in the city, the tourist visits and enjoys the traditional places such as: El Mercado de la Merced, where they could taste the traditional Hornado; the Hispanic churches, such as La Catedral, San Alfonso, la Capilla of San Felipe high school, among others.

Also, Riobamba hosts many important edifices for the history of Ecuador such as El Convento de los Padres Dominicos de la ciudad de Riobamba, nowadays know as Colegio Pedro Vicente Maldonado, where the first constitution of Ecuador was signed; Villa Maria neighborhood, which was installed by whom works in the Misión Geodésica Francesa. All these architectural structures shape an interesting trip for the tourist. However, new structures like homes and another kind of new buildings, which are mostly affected by haloclasty turns less attractive at the city by the eye of tourism.

Although the deterioration of architectural structures associated with salt growing is a common problem in Riobamba City. Any study about this problem has been carried out. In many cases the presence of salts is confused as fungus attack. The study of the deterioration process related to salt growing is a complex phenomenon. In this phenomenon are involved

many variables such as kind of aggregates employed in the different mortars and concretes, environmental conditions, kind of soils present, quality of water, and anthropogenic pollution, among others.

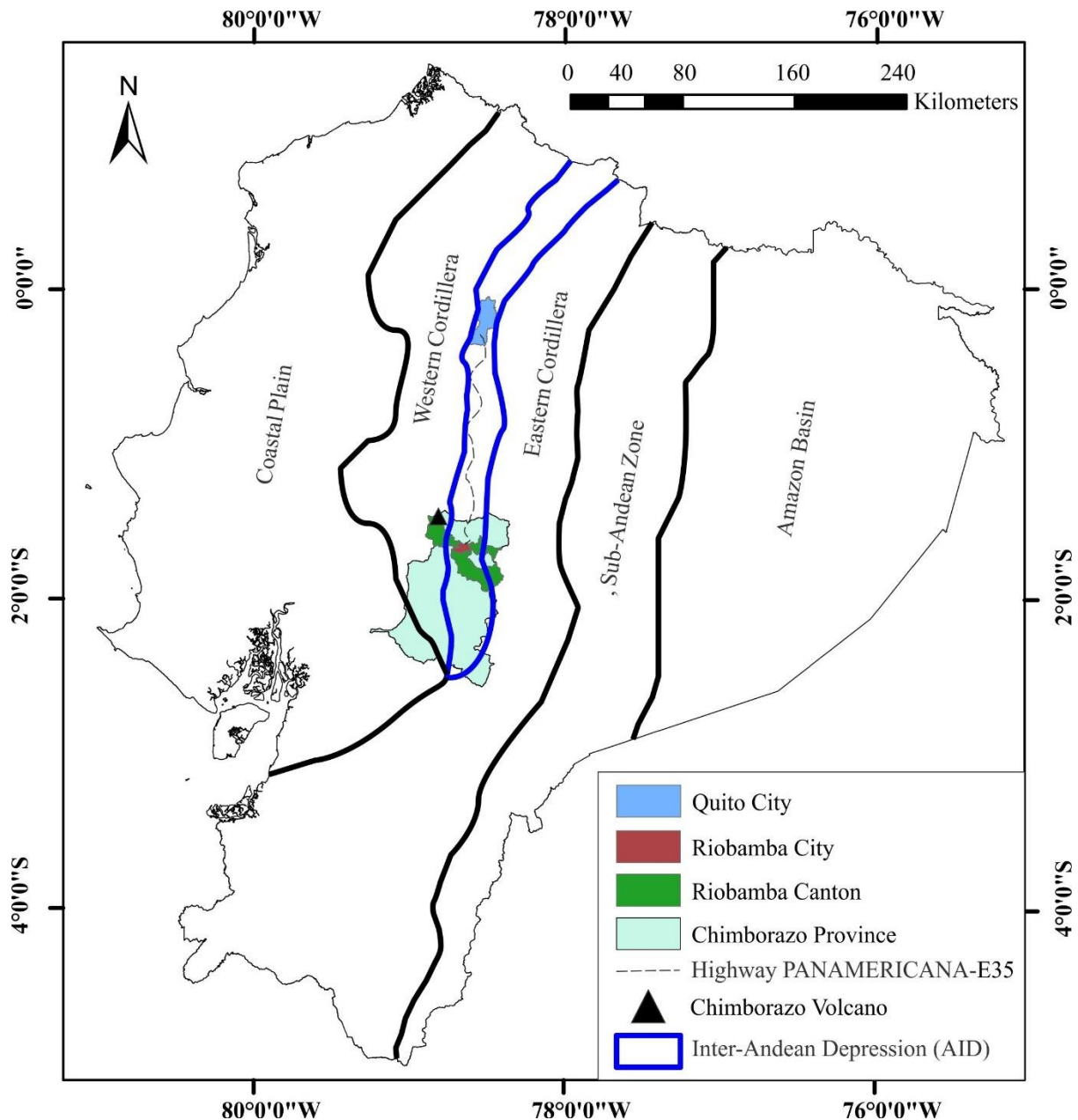


Figure 1. Ecuadorian Tectono-Stratigraphic Regions. The figure shows the six tectono-stratigraphic regions, that conform Ecuador. From oldest to youngest these correspond to: Amazon Basin, Sub-Andean Zone, Eastern Cordillera, Inter-Andean Depression (AID), Western Cordillera, and Coastal Plain (Winkler et al., 2005). Riobamba city, the capital of Chimborazo province, is located in the south of the AID at 211 km, through the highway Panamericana-E35, with respect to Quito City (capital of Ecuador). The Chimborazo volcano is placed in the Western cordillera and represents one of the most important tourist attractions of Riobamba Ecuador.

2 Objectives

2.1 General Objective

Determine the incidence of physical weathering by salt growing deterioration process, haloclasty, and his association with the aggregates employed in the architectural structures of the Riobamba City.

2.2 Main Objectives

- Document the physical weathering problem on the architectural structures in Riobamba city.
- Characterize the deterioration process associated to salt growing.
- Characterize the aggregates employed in the different mortars and concretes used in the architectural structures. Likewise. Characterize the sources areas from these aggregates come from.
- Finally, Determine the minerals phases responsible of the deterioration process, the natural conditions necessary for their formation, and his relationship with the aggregates.

3 Theoretical framework

3.1 Weathering

Weathering is a natural process that consist in: dissolution, disintegration, change in mineralogy, rock to become soil, or soil to become hard layers. The literature identifies three kinds of weathering: mechanical or physical, chemical, and biological weathering (Hack, 2020).

Weathering is a fairly slow process, that produces small changes in very small quantities of material. These changes are the result of the action of atmosphere, hydrosphere, biosphere, and by nuclear radiation over a material. In engineering construction, this proses could jeopardize the structures in a relatively short time. In general, the weathering process take in place on the surface of the ground material. Nevertheless, this could affect deep inside the rock around faults, joints, cracks and microcracks that allows the percolating water (Hack, 2020; Price, 1995).

The main actor that releases the weathering phenomenon in general terms is the energy supplied at the mass (rock). This energy is supplied in many forms but the most important are radiation, temperature, and mechanical forces as strain and stress (Price, 1995).

Each kind of weathering is explained continuously. However, Biological weathering is omitted because: Although biological weathering originated from living beings such as plants and animals. The way of action of this weathering is analyzed and included in the mechanisms of physical and chemical weathering (Hack, 2020).

3.1.1 Chemical Weathering

Chemical weathering results from chemical changes in the mineral composition of a material. These changes are the result of chemical reactions between minerals and weathering agents as water. The chemical reactions responsible of the formation of salts occurs into the water. These reactions depend of the amount of cations and anions solved. Likewise, these also depend on environmental conditions such as temperature and moisture (Price, 2000).

The liberation of acid gases at the atmosphere or pollutants in groundwater, with the reaction with substances realized by biotics (plants, bacteria, animals) produce chemical reactions that can also considered chemical weathering (Hack, 2020).

The susceptibility or endurance of minerals to be weathered depends on the crystal structure (lattice) and chemical characteristics. In general, the minerals result from chemical weathering corresponds to clays. The chemical reactions caused by the man-action as pollution produced by the liberation of gases in the atmosphere or pollutants in ground water, in addition, with the reaction with substances realized by biotics (plants, bacteria, animals), are also consider chemical weathering (Hack, 2020).

In concordance with the environment many chemical reactions produce different kind of minerals. A clear example of this is the formation of mirabilite $\text{Na}_2\text{SO}_4 \cdot 10\text{H}_2\text{O}$ or thenardite Na_2SO_4 . Both are sulfate salts, the difference is that mirabilite corresponds at the hydrated form of the salt, on the other hand, thenardite corresponds to the anhydrate form. The formation of the first one depends on high wet conditions. Meanwhile, the second one depends of dry conditions own of arid environments (Herrero et al., 2015).

3.1.2 Mechanical or Physical Weathering.

Physical weathering corresponds at the process when groundmasses turn in small fragments in a progressively way maintaining the same components (chemical composition), by the action of internal and external forces (Hack, 2020). These forces are the result of many phenomena that take in place in surface or inside the ground, the main phenomena correspond to temperature variations, wetting and drying seasons, freezing and thawing, inside pores overpressures caused by (re-) crystallization, hydration of salts, swelling and shrinkage of minerals due to water absorption (Panchuk & Earle, 2015). In addition, some external forces as the result of the action of biotic agents as the grow of roots or stress and traction caused by the walk of animals. The physical weathering caused by the action of salts is known as haloclasty (Hack, 2020; Panchuk & Earle, 2015).

By a better compression about weathering, it is important to understand the mechanical behavior of the materials.

3.1.3 Mechanical Behavior

The mechanical behavior of a material corresponds to the resistance of this to be deformed against the action of external and internal forces (Price, 1995). To determine the behavior of a material, this is submitted by a tension and compression test which a measured sample is submitted to the action of stress (or loads) and strain (changes in dimension) looking for the point where the sample breaks (Torraca, 2005).

Any material under the actions of forces is deformed, and this deformation could be ductile, elastic or brittle (Price, 1995). According to Torraca (2005) the behavior of materials like stone, mortar and brick is considered as brittle (could be: hard, rigid and fragile). In brittle materials mainly occurs irreversible deformation. This is because by the tendency of the material to nucleation of microscopic cracks and pores under the action of stress. Brittle materials resist better against compressive stresses than tensile stresses (Price, 1995). Depending on the origin of the stress this could be external or internal.

3.1.3.1 External Stress

This kind of stress is produced by the action of external factors that could exert strain (tensile), traction, and or stress (Torraca, 2005). Among the mechanisms by which internal stresses is originated are the following:

Load: Any civil structure is designed to minimize tensile stress and allow materials to work mainly under compression (columns, lintels, pillars). The major deterioration present in a building corresponds at a zone that is affected by a particular kind of stress known as tensile stress (Torraca, 2005).

Thermal Expansion: This phenomenon corresponds to the tendency of materials to deform as a result the daily and seasonal climate conditions. The deformation over a material depends of change in temperature, by high temperatures materials expands (dilatation), on the other side, under low temperatures materials contracts. In addition, the length of the deformation is directly proportional to the length of the material. The restriction, of materials inside a building, to dilatation or contraction produces microcracks, cracks and future deformations. The microcracks and cracks are permanent, and they do not close angina even after the contraction process. Finally, the rate of deformation varies between materials, and this depends of the thermal expansion coefficient (Torraca, 2005).

Expansion due to Moisture: This phenomenon corresponds to porous materials that expands where these pores absorbers water ant contract when release its. The damage produce by moisture could be neglected in comparation with damages produced by thermal expansion. Likewise, this phenomenon is important for materials that contain clays (Torraca, 2005).

Stress caused by Working Techniques: This corresponds at cracks (could be micro-cracks) that are originated when the material is structed or prepared to be employed in a building. Some techniques of extraction like the use of dynamite in quarries, in addition, cleaning methods cleaning methods like grit blasting or scratch brushing can produce mechanical damage (cracks) on the surfaces. However, techniques of polish over stone turns it stronger against deterioration, due to the deterioration rates is directly depended of the mechanic surface condition. Grade (Torraca, 2005)

3.1.3.2 Internal Stress

The internal stress is a force produced inside the pores of the material because of the interaction between crystals and water (Price, 2000). Inside the material the stress caused by crystals interaction is balanced by the resistance to compression of the material around them. However, in the surface there is not this resistance as a result the pore breaks turns weaker at the surface and turning it easier to be deteriorated (Torraca, 2005). Among the mechanisms by which internal stresses is originated are the following:

Frost: This phenomenon corresponds at the formation of ice inside the pores. In general, ice crystals only grow inside big voids (large pores or fractures) however, ice could be present inside little pores as the action of pressure. Pressure is the result of water presence after the growing crystals by water feeding (Torraca, 2005).

The damage upon material produced by frost does not depends on the expansion that suffer water when it turns in ice, it depends on the size of the pores. Smaller pores in the order of 0.1 to 1 micron could rise the stress (Torraca, 2005).

Salt Crystallization: There are two models to describe the stress originated by this phenomenon. The first model takes in count the size of the pores. Crystals grow or are deposited by the action of water. When crystals fill up the large pores or fractures, the remained crystals content in water solutions are deposited inside little pores (0.1 to 1 micron) originating a high pressure capable to break the pores (Torraca, 2005).

The second model corresponds to hydrated salt crystals. Molecules of water inside salts occupy a specific place in the crystal structure. Molecules of water according to the environmental conditions could be inside (hydrated salt) or outside (anhydrous salt) the crystals. At conditions of high temperature or low humidity the water tends to escape from the crystal. The total volume of a hydrated salt is smaller than in comparison with the total volume formed by water and the anhydrous salt separately. This difference between volumes produce stress over the pore walls (Torraca, 2005).

3.1.4 Haloclasty

Haloclasty is a kind of physical weathering characterized by crystallization of salts. Around the world salts are the major contributor in the deterioration of porous materials being

particularly affected those are employed in the construction of architectural structures such as: mortars, terracotta and concrete bricks (Torraca, 2005).

The physical damage caused by salts is the result of an overpressure ejected by salts inside the pores (Haynes, 2002). This pressure may originate from the following phenomena: crystallization of salts from supersaturated solution, changes in the hydration state of the salt, and chemical reactions. The phenomenon causes a powdering and granular disaggregation of the surface, posterior, a gradual loss of the surface. In other cases, this manifests itself in form of surface scaling, similar in appearance to that caused by freezing and thawing damage (Haynes et al., 1996; Torraca, 2005).

The field tests carried on Sacramento, California, in 1940 correlate the formation of salts with flood conditions. To recreate these conditions the Portland Cement Association (PCA) dipped bottom of concrete slabs in a solution at molarity of 10% of sodium sulfate, six to eight times in a year. As a result, in the dipped zone the sulfate crystallization and the posterior deterioration of the slab was evident (Haynes et al., 1996).

3.1.5 Mechanisms of Salt Damage

According to Torraca (2005), the total mechanism of salt damage over porous materials corresponds to a particular combination between the action of stress and corrosion that affects the mechanical behavior of materials. Stress and corrosion are the result of chemical process that taken in place on the surface as well as inside the material.

3.2 Salt Damage in Architectural structures

In architectural structures the damage by salt crystallization is present in many forms of weathering such as tafone, honeycombs and pedestal rocks, as well as mortar or concrete debris. This phenomenon is often misidentified as sulfate attack. Sulfate attack is considered to be distress caused by the formation of ettringite ($C_3A \cdot 3CaSO_4 \cdot 32H_2O$) and gypsum ($CaSO_4 \cdot 2H_2O$), as a result, of chemical reaction between the sulfate ions and the hydration products of Portland cement. The reason sulfate attack is a misidentified term is that the term encompasses the mechanism where sulfates and non-sulfates are involved (Doehne, 2002).

The classic mechanisms by sulfate attack includes the following cases: Gypsum formation by hydrated external ions of sulfate (soil, or groundwater) and calcium ions from

cement; Ettringite formation by hydrated external ions of sulfate (soil, or groundwater) in addition with alumina and calcium ions from cement (Doehne, 2002).

In addition, the non-sulfate mechanism of attack considers the rest of salts involved and process involved in the weathering process. The most common non-sulfate involved salts corresponds to carbonates nitrates, chlorates, phosphates ((Dalton et al., 2022; García-Florentino et al., 2016). Likewise, this mechanism takes in count different process also related to the weathering such as: Sulfuric acid production by the oxidation of iron sulfide in sulfate; Decomposing of magnesium sulfate in magnesium cations from cement paste and the physical attack caused by sodium sulfate (Doehne, 2002). Both mechanisms are studied individually since the damage associated with the first one (sulfate attack) is much greater than the second one (non-sulphate) (Doehne, 2002).

4 Geology and Weather Framework

4.1 Regional geology

Ecuador is formed by six different tectono-stratigraphic regions. These regions listing from east to west corresponds to: Amazon Basin, Sub-Andean Zone, Eastern Cordillera, Inter-Andean Depression (AID), Western Cordillera, and Coastal Plain (Figure 1). This way of listing gives the order of formation of each domain too (Winkler et al., 2005).

The Amazon Basin corresponds to a slab of Proterozoic metamorphic rocks that eastward extends, overlain by sedimentary and volcanic successions from the Paleozoic and Mesozoic, and a posterior sedimentary deposition. Sub-Andean Zone is over the western margin of the Amazon Craton that corresponds a Jurassic volcanic arc basement. Over this is emplaced sediments from the Quaternary. The four westernmost tectono-stratigraphic regions accreted in the continental margin of the South American Plate between the Late Jurassic and the Late Cretaceous. The data show the presence of an allochthonous oceanic mafic plateau as basement of Coastal Plain and Western Cordillera. The Inter-Andean Depression was formed by differential uplift and thrusting of the cordilleras at 6-5Ma ago (Chiaradia et al., 2009; Ruiz et al., 2007; Vallejo et al., 2006).

From the six tectono-stratigraphic regions listed previously, the Inter Andean Depression the great importance because the study zone (Riobamba city) is placed here (Figure 1).

4.1.1 Inter Andean Depression

The inter-Andean Depression (AID) corresponds a row depression below 3 000m of high, oriented NNE to SSW, flanked in the east by the Eastern Cordillera and the Western Cordillera to the west. This was formed as the result of tectonic rearrangement of the Ecuadorian Andean forearc and arc (late Miocene). In Ecuador AID extents approximately since 0°45'N until 2°30'S (Figure 1). From north to south AID is formed by the following sedimentary sub-basins: Chota basin; Quito-San Antonio-Guayllabamba basin; Ambato-Latacunga basin; and Riobamba-Alausi basin. The different sub-basins are dated in a range between the latest Miocene to Pleistocene. The geological structures that limit the AID correspond to: at the east the Peltetec fault, formed the accretion of the Eastern cordillera (late Jurassic), and the Pallatanga-Pujil-Calacali fault in the west, formed by the accretion of the

oceanic Pallatanga terrain (late Cretaceous). The southern zone of the AID extends westward south toward the Gulf of Guayaquil dissecting the Western Cordillera parallel to Pallatanga-Pujil-Calacali fault (Winkler et al., 2005).

Over the Chota sub-basin lies a sedimentary sequence of 1200 to 1400m thick, which is divided by a lahar sheet in two geographically parts. In the eastern and central part, the Peña Coloradas formation (volcano-sedimentary sequences). Later, to the west, in a fluvial to lacustrine environment was deposited the Chota Formation formed by sandstones, andesitic and basaltic volcanic rocks (folded sills and dikes) and lies over the Pallatanga unit. (Winkler et al., 2005).

Southward, it is located the Quito-San Antonio-Guayllabamba sub-basin over the Pallatanga unit. Over this lies a succession of volcano sedimentary formations (Pisque, San Miguel, Guayllabamba, Chiche, Mojanda and Cangahua formations) (Winkler et al., 2005).

The Ambato-Latacunga basins is covered a succession of volcanic to volcanoclastic rocks deposited in a fluvial to lacustrine environment (Sicalpa, Latacunga, Chalupas formation) (Winkler et al., 2005).

Finally, the Alausi-Riobamba basins that corresponds the southern termination of the Ecuadorian arc, lies over the Pallatanga unit and it is composed of two formations. The Huigra formation (Saraguro Group) in the north, and the Alausi formation (Turi and Traqui volcanic formations) in the south, both covered by a sequence of alluvial fan and fluvial conglomerates that forms the Palmira and Sicalpa formations, in addition, with volcanic and volcano-sedimentary deposits related to: pyroclastic flows, debris, and lahars. These the volcanic and volcano-sedimentary deposits correspond to Debris Avalanche Deposits from Chimborazo volcano (DAD) deposited as the result to the collapse of the basal edifice of Chimborazo volcano (Samaniego et al., 2012; Winkler et al., 2005)

Bernard et al., (2008) classify the debris avalanche deposits from Chimborazo volcano (DAD), or Chimborazo Unit (PICH1), in three zones according to his proximity to Chimborazo volcano and these are the following: i) the proximal zone that covers an extension of 135 km², ii) the medial zone covering a surface of 95 km², iii) the distal zone emplacement in an area of 50 km² (Salguero, 2017).

The deposits present in Riobamba city corresponds at the medial zone of the DAD. This corresponds to debris deposits of 40 m average thickness from the Chimborazo volcano (Bernard et al., 2008). Samaniego et al., (2012) define this zone as The Riobamba debris avalanche deposits (R-DAD) (Figure 3).

4.2 Local Geology

According to the Strategic Cantonal Development Plan by 2025, Riobamba City is in the north center of the Chimborazo province. The city covers an approximately area of 28.13 km². The average altitude corresponds to 2 754masl (EP EMAPAR, 2018).

The local geology corresponds a basement composed of sequences of quartzites and slates from the Guamote unit also know like Cevadas or Punin unit. Over these sequences was deposited volcanic and volcanic-sedimentary material from the eruptive process of specially from Chimborazo volcano (Bernard et al., 2008). The material deposited in this zone posteriorly will conform the geological units described by Sosa, H. & Guevara, S. (1973), in the Riobamba Geological Chart 1:100 000. Among the lithological units that outcrop in the city are contained the following: Riobamba unit, Yaruquies formation, Sicalpa unit, in addition, the quaternary deposits that corresponds to Terraces and Alluvial deposits (Bernard et al., 2008 y Samaniego et al., 2012). These sequences were deposited during a compressive regimen caused by the subduction of the Nazca plate. This produced high rate of exhumation of the Eastern Cordillera (Buenaño, 2018).

4.2.1 Lithological Units

The different lithological units that outcrop in the city listed from old to young correspond to the following.

Macuchi Formation: In the most recent studies carried by Vallejo. (2007), suggest that Macuchi Unit corresponds to submarine volcanic arc of calc-alkaline and tholeiitic chemical composition, deposited during the Paleocene to Eocene. The lithology of this unit mostly corresponds to volcanoclastic bed deposit (pillow lavas, lithic tuffs of basaltic and andesitic composition), and to a lesser extent in basaltic breccias that corresponds to polymictic breccias composed by angular clasts of dacites, andesites, basalts contained in an epidotized andesitic matrix with high amount of glass.

Yaruquies Formation: This formation is described as an inverse graded sequence of fluvial kind. This formation outcrops at the south of the city. In the base, the strata have a thickness of 50 cm. This corresponds to a matrix supported deposit. The matrix is composed of silt grain size. The clasts correspond to sub-rounded andesites and dacites with an average diameter of 30 cm. The top of the sequence corresponds to an alternation of conglomerates, sandstones and shales. This formation was dated from 24.6 ± 1.33 Ma (Miocene). In addition, the geochemical characteristic of this formation shows that these sediments were deposited in a continental active margin (Cobos et al., 2022; Noblet et al., 1990).

Altar Unit (PL_{AL}): The Altar unit was dated from the Pliocene. This unit is considered as avalanche deposit emplaced posterior to the collapse of the Altar Volcano. The lithology consists in a light gray to beige, massive volcanic breccia, emplaced in a matrix of medium to coarse sandstone grain size. The volcanic breccia corresponds to sub-angular blocks of size less than 2 m. This breccia is composed by volcanic lithics of andesitic composition. The main minerals in the lithics corresponds to plagioclase and hornblende phenocrystals (Salguero, 2017).

Sicalpa Unit (PL_{SI}): In Riobamba city the Sicalpa unit (PL_{SI}) is located in the southwestern zone in the limit with Calpi town. PL_{SI} has a thickness that varies from east to west between 20 to 40 m. This unit correspond a sequence of volcanic deposits composed by tuffs, volcanic conglomerates and lava flows, from different volcanic events of the Chimborazo, Altar and Tungurahua. The strata are described as a massive conglomerate of gray-dark to rosaceous-gray color. The clasts show porphyritic texture, its mineral composition corresponds to plagioclase, pyroxene, amphiboles, and some clay minerals as result of low argillic alteration. This textural characteristic in this unit means that was deposited in a secondary lahar event, and it is dated from medium Pliocene (Salguero, 2017).

Riobamba Unit (R-DAD): This Unit corresponds as a debris avalanche deposit (DAD) composed by volcanic and volcano-sedimentary material from the collapse of the CH I edifice of Chimborazo volcano (Clapperton, 1990).

The R-DAD placed in the Riobamba valley is described as two facies. The predominant facie corresponds at the block facies. This is described as clast-supported deposits formed by diaclosed blocks bigger than 5 m² with placed in matrix composed by grains of size between sandy to silty. The kind of rocks found here corresponds to two-pyroxene andesite, pyroxene

andesite, amphibole andesite, pyroxene-amphibole andesite, amphibole-plagioclase andesite rocks. The second facies correspond to the mixed facies. This is matrix supported deposit. The matrix is composed by brains of sandy-silty size. Inside the matrix are contained few blocks with the same lithology as block facies. Also, it is possible to find substratum material such as: clay rocks, ashes, and pebbles. Finally, there is not a direct dating from these facies. However, how these facies overlaying volcanic deposits dated at ~68 ka, them is supposed that these were deposited after this date (Bernard et al., 2008; Samaniego et al., 2012).

Quaternary Deposits: According with the IGM (2012) in the project: “GENERACIÓN DE GEOINFORMACIÓN PARA LA GESTIÓN DEL TERRITORIO A NIVEL NACIONAL ESCALA. 1: 25.000” the quaternary deposits composed by fine to medium clays and sand with presence of fine gravel, in addition with silts. These deposits according to their morphology are classified in: Alluvial Deposits, Terraces and Landslides (Figure 2) (MAGAP, 2012).

4.3 Weather of the Region

Ecuador is in the tropical region of the planet. This region extends from north to south since the tropics of Cancer (23.5 °N) until the tropics of Capricorn (23.5 °S). At the tropical region are associated high temperatures and air humidity. However, these can change by the action of different factors such as: altitude, topography, wind patterns, ocean currents, geomorphology, vegetation and, more recently by large scale manmade environmental changes (Val et al., 2005).

The continental Ecuador corresponds of three main regions Coast, Andean, and Amazonian. These three regions are possible thanks to the presence of the Andes. The Andes cross Ecuador form north to south (Palma-Henríquez, 2018). From the tectono-stratigraphic point of view the Coast corresponds to the Coastal Plain. The Andean is formed by the Western cordillera, Inter-Andean zone, and Eastern cordillera. And finally, Amazonian corresponds to Sub-Andean zone and Amazon basins.

From these three main regions is the important interest the Andean region, because Riobamba city is located here. The Andean region is composed by four different kinds of climates. These climates are classified according to the next parameters: raining seasons, altitude, precipitation rate, temperature, and humidity. In base of these parameters the climates in the Andean region correspond to the following:

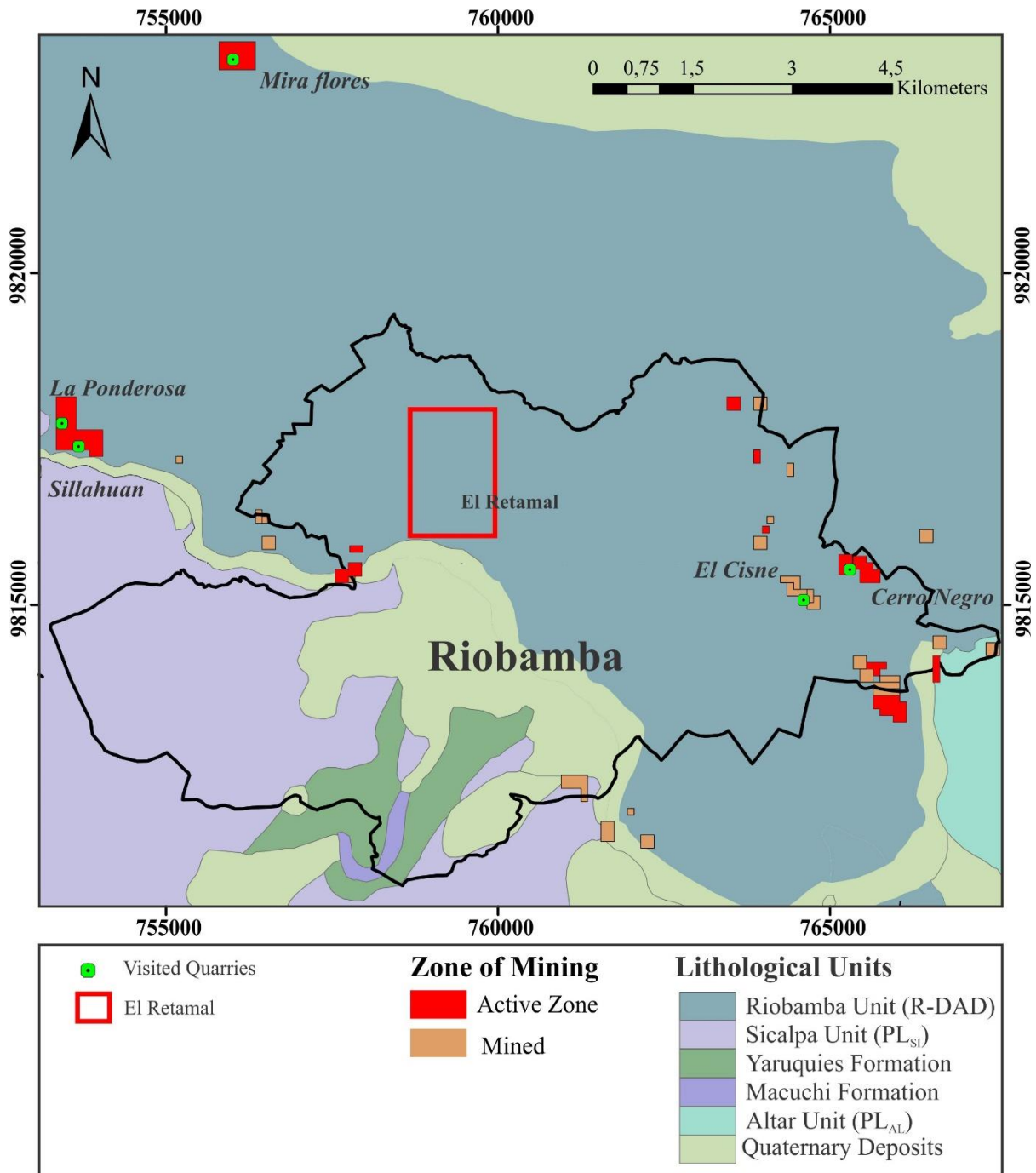


Figure 2. Geological Map of Riobamba City. This map shows the special distribution of the different geological units presents in the city. The Riobamba Unit R-DAD is the predominant and emerges the north and east of the city, the rest emerges at the south-west. The red and orange rectangles show the areas designed for mining y the municipality of Riobamba through the time. From these, red rectangles show the zones that still working. The map also shows the specific location of each quarry visited by the development of this project IGM (2012).

- Semi-humid to humid mesothermal equatorial climate: This kind of climate is characterized by two raining seasons during the year. The average temperature and relative humidity (RH) vary from 12 to 20°C and 65 to 85% respectively. In addition, the highest and coldest temperatures registered are 30°C and 0°C.

- Dry mesothermal equatorial climate: This kind of climate as the previously is characterized by two raining seasons. The average temperature varies from 12 to 20°C. However, relative humidity (RH) only varies from 50 to 80%.
- High mountain cold equatorial climate: This climate is typical of heights greater than 3000 m. The average temperature is 8°C rarely arrives at the 20°C, and the RH always is above to 80%. This climate is also characterized by two different raining seasons.
- Very humid tropical mega-thermal climate. The average temperature is 8°C rarely arrives at the 20°C, and the RH always is above to 80%. This corresponds at the climatic conditions present in the transition zones between the Coast with the Andean region, as well as the Andean with the Amazonian. The average temperatures around the year are high, likewise the RH is always around to 90°C (Pourrut, 1983).

The average temperature in Riobamba varies from 8 to 19 °C, however, in many cases the maximum temperature can arrive until the 22 °C. The precipitation in this region is bimodal. The first and most intense period occurs from February to May. The second and less intense period begins in October and ends in December. The first period is caused by the influence of the air masses from the Pacific Ocean, and the second for masses from the Amazonian. The average precipitation in the region corresponds to 450-800 mm year⁻¹ (Ilbay-Yupa et al., 2021). Finally, the RH in base of data from the weather station RIOBAMBA-POLITECNICA varies from 68 to 77% (INAMHI, 2017).

5 Architectural structures in Riobamba City

According to Instituto Nacional de Estadísticas y Censos, Inec. (2011) the total architectural structures in the urban zone of Riobamba city corresponds a total of 31 254. These architectural structures from the architectural point of view are classified in two groups. The first one corresponds to the historical heritage buildings, and the second corresponds to republican buildings (Lemache, 2017).

Are consider as historical heritage buildings to which that have an historical value for the society and must be protected and conserved for the future generations (Vecco, 2010). In concordance with Lemache (2017) the heritage buildings in Riobamba are Gothic or Romanesque style, influenced by the Italian, Anglo-Saxon, and French architecture (Figure 3). These structures were built employing volcanic blocks, bricks, wood, and rammed earth. In Riobamba there are 435 structures recognized as historical heritage buildings which are located specially in the historical center of the city. (RIOBAMBA – Ministerio de Cultura y Patrimonio, 2022).



Figure 3. Historical Heritage Buildings of Riobamba city. La Catedral church, Edificio del Correo, Municipio de la ciudad de Riobamba and La Basilica church. Architectural structures of Gothic stile (Author).

The republican buildings correspond to modern structures built in base of cement, bricks, sand and iron [Figure 4 a)]. The total amount of this king of buildings in the city is 30 819 according with the data form Instituto Nacionala de Estadisticas y Censos (INEC 2011). In an interview with the civil engineering Pablo Criollo, he enunciates the following: form the engineering point of view, according with the state or condition in which the building ends, these could be classified in base of the next parameters:

- White work buildings: If the buildings are composed by concrete or terracotta bricks walls covered by a film of mortar followed by a shell of plaster, or paintwork, or both [Figure 4a)].
- Gray work buildings: If the buildings are composed by concrete or terracotta bricks walls covered by a film of mortar [Figure 4b)].
- Black work buildings: If the buildings are composed by concrete or terracotta bricks walls exposed directly to the environment [Figure 4c)].



Figure 4. Republican Buildings in Riobamba city. The figure shows the typical republican buildings and its classification according to the ending of the building. a) shows a typical republican building built in base of concrete, bricks, iron, and aggregates. Likewise, a) is a white work building because the walls are cover by a white plaster and painted b) this picture shows a building where the ground floor corresponds a white work. However, the upper floors are designed as gray work building due to, the endings correspond a wall cover by mortar without protection against the environment. Finally, both walls showed in c) there are two different black work building because bricks (terracotta, concrete) and columns does not have any protection (mortar, paint) against the environment (Author).

6 Methodology and Materials

The following Chapter shows the methodology and materials employed in this project, beginning with the description of the different built materials employed. Posteriorly, it is shown the criteria employed to take the samples. Finally, relate the steps taken in place on the laboratory to determine the mineral phases responsible of the civil infrastructure deterioration.

6.1 Building materials and their provenance.

How was enunciated previously the majority of buildings in Riobamba corresponds to republican buildings. These kinds of buildings use as raw material bricks, cement, iron rods, aggregates (sands and stones), and water [Figure 4 a) and b)]. The most common is that the materials which by employed in the buildings be bought from near zones due to this reduce the time and cost of transport.

Bricks: The bricks employed in the republican buildings are of two kinds of bricks, terracotta bricks and concrete bricks. Each kind of brick is elaborated based on the specifications dictated in NTE INEN 2380 (2011).

Terracotta brick is the most used in construction due to its mechanical properties that provides denser walls capable to support high stresses. This kind of bricks are defined as ceramic pieces composed by clay or loamy soil mixed with water and sometimes with other plastic materials, but these must be in a low proportion, forming a paste. This paste is placed in molds whose dimensions are 29 x 14 x 9 cm, where the paste rest until solidified, forming blocks. Posteriorly, these blocks are baked in an oven at a minimum temperature of 800° C, obtaining as a result massive uniform ceramic block of terracotta color (Figure 5a). The most common precedence of terracotta brick employed in Riobamba corresponds to craft factories located in Chambo canton (Gavilanes & Santellan, 2016).

Concrete bricks correspond to great resistance compression blocks composed by Portland cement, sand and water, forming a past that is placed in molds with dimensions of 15x20x40 cm, its shape corresponds to hollow blocks inside without a plane of 15 x 40 cm. The paste solidifies in a minimum time of 28 days when it reaches its maximum resistance and obtaining its characteristic gray color (Figure 5b). The sand employed in this is extracted from the quarries of the city specially from Cerro Negro. In Riobamba there are many craft factories which spends this kind of bricks. (Romero & Chuquimarca, 2011).



Figure 5. *Terracotta and Concrete Bricks. a) shows the form of terracotta bricks employed to build the different infrastructure in Riobamba city. b) shows the form how concrete brick is exposed to be expended (Gavilanes & Santellan, 2016).*

Iron rods: These consist in large iron cylinders which diameter varies in a range between 8 to 40 mm, according to the needs of the building. Iron rods are employed in the reinforcement of structures that could be concrete columns or slabs (Figure 6). The biggest distributor of Iron rods in Ecuador is Adelca company (Adelca, 2020).



Figure 6. *Iron Rods. Iron rods structures employed to enforce slabs and columns. These structures are directly cover by concrete (Adelca, 2020).*

Cement: According to Instituto Ecuatoriano de Normalización in the NTE INEN 2380 (2011), the cement employed in general for buildings, that does not need special specifications, corresponds to hydraulic cement of GU type. This is a kind of Portland cement that reacts with water to form solid mass. Portland cement according the American Concrete Institute “is the product obtained by pulverizing clinker, consisting of hydraulic calcium silicates to which

some calcium sulfate has usually been provided as an inter-ground addition” (American Concrete Institute, 2022.). The chemical composition of the Portland cement is expressed in form of oxides CaO, SiO₂, Al₂O₃, Fe₂O₃, where could be included other materials, but in a very low proportion (Orna, 2019). In Riobamba the most important companies that spend hydraulic cement UG type corresponds to: Cemento Chimborazo, and Holcim Ecuador (Figure 7).



Figure 7. Holcim and Chimborazo Cement. The figure shows the typical presentation of the 50kg bag of Hydraulic Cement Type GU from the most important companies Holcim and Cemento Chimborazo. According with the normative of construction of Ecuador the GU type cement must be employed in general for buildings that does not need special specifications.

Aggregates (Sand and Stones): These commonly called arid and stony, or simply aggregates, corresponds at the material mined in quarries, and these are classified according its grain size. The quarries mined material specially from the Riobamba Unit (Figure 2). The aggregates correspond at the materials that are used in greater proportion within the architectural structures. The aggregates expended corresponds to fine sand, medium to coarse sand and gravel (ripio).

The way of mining corresponds an Open-pit mine (Figure 8), where the material is removed employing heavy equipment forming terraces. Posteriorly, this material is transport in dump trucks toward the zones where will be processed. And finally, the material is classified to obtain the different kind of sands and stones to be commercialized posteriorly (Figure 8).

The fine sand is sold by the preparation of mortars that will be employed in the endings of the buildings. In other words, this mortar is used to cover walls and concrete columns. The medium to coarse sand is employing in mortar used to join the bricks in walls. And finally, the shredded clast is used in the concrete employed in slabs and columns.



Figure 8. Mira Flores Quarry. The figure shows a typical quarry in Riobamba city. This quarry corresponds to Mira Flores and it is located at the north of the city in the Panamericana E-35 highway. In the background of the image, it is possible to see how heavy machinery mined the material from the deposit. This material posteriorly is sifted to be expended at the citizens (Author).

Water: The water employed by the citizens of Riobamba coming from underground sources (Muñoz, 2020). The source is extracted by bombs installed in wells that suck the water toward the surface. The water from wells is carried to a treatment plants and posterior to the different reservoirs located in the city. How all the water comes from the same treatment plant, the water in all the city has the same characteristics (Mancheno, 2010).

The chemical properties of water were analyzed by Muñoz (2020). The analysis was carried on each well that supplies of water to Riobamba city. The results show that the sulfate content solved in water varies from 8 to 480 mg/L, and nitrates from 1 to 3.4 mg/L. The detailed chemical characteristics of water is described in the Anexe 1.

6.2 Sampling

Due to Riobamba city covers an area of 59.05 km², a sampling process that covers all the city was no possible. For this reason, the sampling was development in the northwest zone of the cite that corresponds to the Lizarzaburu parish, in the sector known as El Retamal (Figure 9). This sector was selected because the zone shows the ideal conditions to the development of this project. In addition, the neighbors are familiar with the researcher and make it easier to take samples.

El Retamal corresponds an important sector of the Riobamba city due to its proximity at the Escuela Superior Politecnica de Chimborazo (ESPOCH) university. This is a residential sector where students of all the country looking for accommodation, while they carry out their university studies.

The sampling process was development in august of 2022 during the dry season. The process consisted in the specifically collection of white minerals that efflorescence in the external walls of the buildings. For the sampling was employed a metallic spatula with which the efflorescence formed in the walls was scraped. Posterior to the scraped, the material was deposited in hermetic plastic bags. After the scraped of each sample the spatula was cleaned employed alcohol and a flannel taken in count that any mineral or flannel particle still upon the spatula, to avoid any type of cross contamination. In total 72 samples were taking across these days (Figure 9 and Annex 4).

In addition, During the 13,14, and 15 of December of 2022 was carried out different filed trips toward the different quarries in Riobamba city (Figure 2). However, only was possible to visit the quarries located in the west, northwest and east, because the quarries in the south are closed and the access is restricted. In the quarries visited was verified their lithology, the way of mining and, the final products that spends (Annex.3).

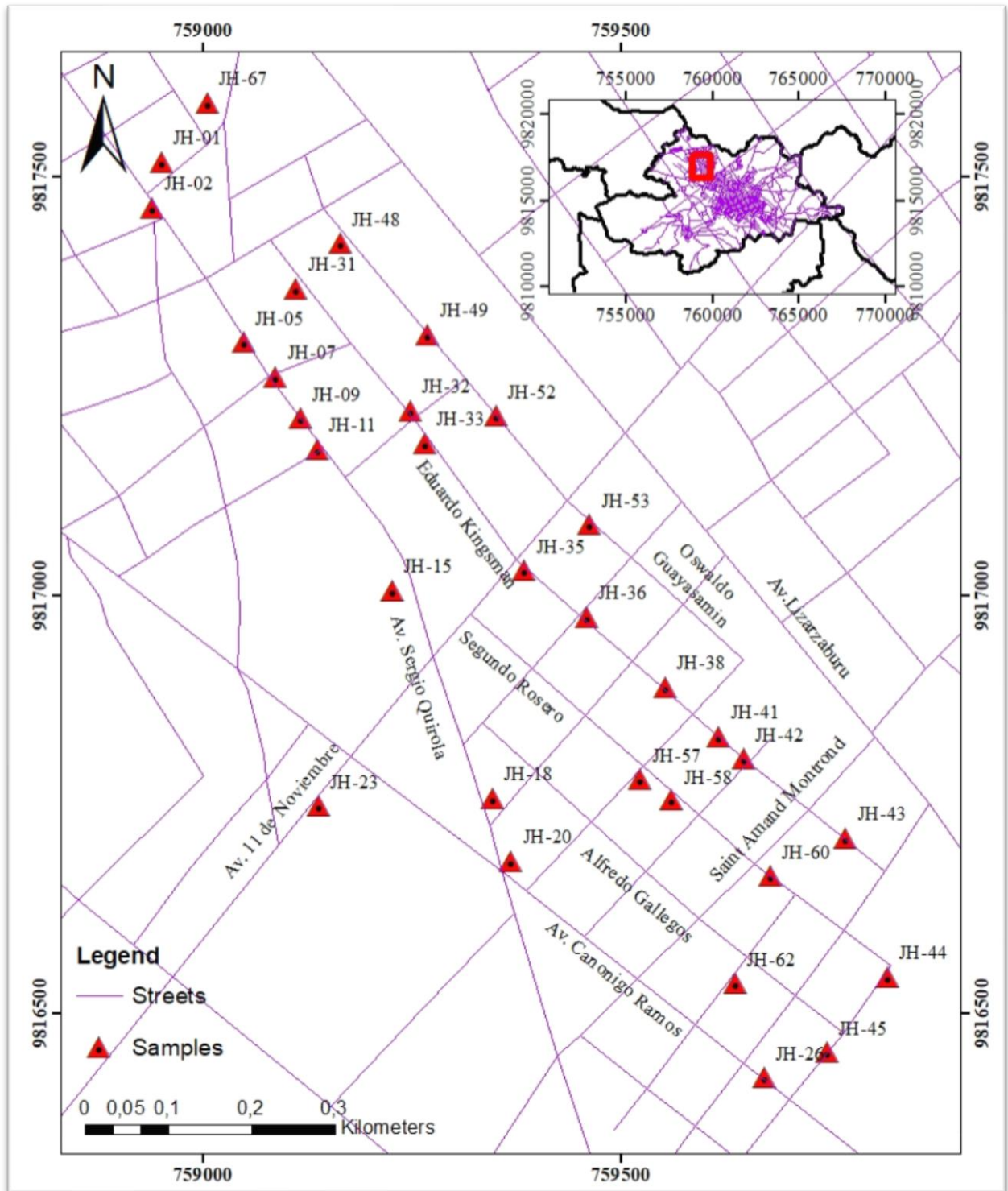


Figure 9. Study Zone. The map shows the northwest part of Riobamba city known as El Retamal. The red triangles show the points where the different samples were taken. The principal streets and avenues travelled corresponds to: Av. Sergio Quirola, Av. 11 de Noviembre and, Oswaldo Guayasamin, Eduardo Kingsman, Segundo Rosero Alfredo Gallegos streets (Author).

6.3 X-ray Diffraction Analysis

The method employed to determine the mineral phases, responsible of the haloclasty phenomenon in Riobamba city, is known as X-Ray Diffraction analysis (XR-D). This method

requires a previous preparation of each sample before being analyzed. Posterior, these samples are analyzed in the laboratory of materials studies from Yachay Tech University. Finally, the data obtained in the laboratory are processed in a software to determine the mineral phases.

Sample Preparation: From the 72 samples taken (Annex 4), only 32 were selected by the analysis. The criteria to select these 32 samples was in base at the location and amount of sample. The specific location of each sample selected for the analysis is present in the table 1.

Table 1. Specific location of the 32 samples selected by the XR-D analysis. The table also shows the structure where the sample was taken.

Sample	Latitude	Longitude	Structure
JH-01	9817517,87	758950,228	Closing brick wall
JH-02	9817463,04	758939,422	Home facade
JH-05	9817302,09	759048,773	Home facade
JH-07	9817261,26	759087,143	Closing brick wall
JH-09	9817211,15	759116,451	Home facade
JH-11	9817174,68	759137,036	Home facade
JH-15	9817005,76	759226,006	Home facade
JH-18	9816757,15	759346,364	Home facade
JH-20	9816682,49	759368,251	Home facade
JH-23	9816747,99	759137,759	Home facade
JH-26	9816423,33	759671,063	Home facade
JH-31	9817366,68	759111,334	Home facade
JH-32	9817221	759247,71	Home facade
JH-33	9817182,15	759265,576	Home facade
JH-35	9817029,77	759384,389	Home facade
JH-36	9816974,17	759458,297	Home facade
JH-38	9816890,6	759552,132	Home facade
JH-41	9816831,1	759616,517	Home facade
JH-42	9816805,45	759646,032	Home facade
JH-43	9816709,65	759768,273	Home facade
JH-44	9816544,14	759818,384	Home facade
JH-45	9816453,78	759745,951	Home facade
JH-48	9817420,73	759163,819	Closing brick wall
JH-49	9817311,61	759268,912	Home facade
JH-52	9817192,83	759321,439	Home facade
JH-53	9817084,15	759462,378	Home facade
JH-57	9816780,14	759522,58	Home facade
JH-58	9816756,3	759560,189	Home facade
JH-60	9816664,39	759678,082	Home facade
JH-62	9816535,85	759636,274	Home facade
JH-67	9817532,63	757723,379	Home facade

The preparation of the 32 samples consists in the manual pulverization of each sample until obtain particles as fine as possible employing a mortar [Figure 10 a)]. The samples must become in a silt grain size (Figure 10a). Posterior, the pulverized sample is placed in molds designed specifically by the XR-D analysis avoid any fissure in the surface of the sample how is showed in the (Figure 10b). Finally, the molds are placed in the XR-D analyzer and the parameters for the analyses are adjusted (Figure 11).

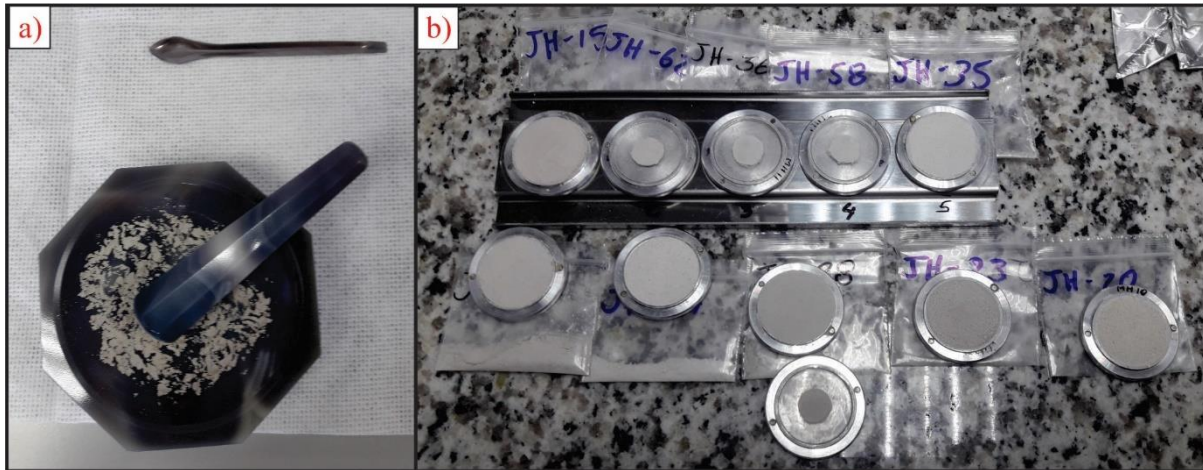


Figure 10. Sample processing: The pictures show the different steps necessary to the samples turns adequate for the XRD analysis. The picture (a) shows the pulverization of the sample, while (b) shows the correct way to emplaces the samples in the molds (Author).

X-Ray Diffraction Analysis (XR-D): This corresponds a physical method employed by the characterizing of solids, developed by Wilhelm Rontgen in 1895. Employing a XR-D analyzer (Figure 11) is possible to quantify the amount of different mineral phases in function of percentages of the total mass analyzed and find many qualitative properties phases such as: types, fingerprint, and crystallinity. This method works in base of the Bragg's law, which correlate the monochromatic light beam that inside over the sample and interacts with the lattice forming by n number or of sheets, and the scattering angle of the beam as result of the interaction.

Nowadays, to solve this equation is used the software Match!, which give a result in form of figure know as interference figure. This interference figure is compared whit an extended data base that contains the standard interference figure specific for each mineral phase. In addition, Match! give the probability of the presence of a specific mineral phase, and a qualitative value in percentage form of this phase in relationship of the whole sample (Abdulrazzak & Alkiam, 2019).



Figure 11. XR-D analyzer from the Yachay Tech university. The samples are scanning in the machine located at the right. Posteriorly, the data is digitalized and saved in the computer located to the left (Author).

Data Processing: The data obtained from the XR-D analyzer is known as Interference figure (Figure 12). This figure is loaded in the software Match!, which allows to improve the quality of the figure, employing the next options:

- Smoothing: This cleans the noise from the interference figure.
- Strip K-Alpha2: This cleans the image of the peaks formed to employ an analyzer that does not use a monochromatic beam.
- Subtract Background: This substrate the base line from the figure and let works only with the principal peaks of the figure.
- Pack Search: The software is responsible for locating the peaks of the figure. Nevertheless, it is recommended to do a manual check and insert the peaks that the software has omitted.

Posterior to clean the interference figure the software make a comparison between this and a data base and give a set of multiple mineral phases that could concordat with the interference

figure. Finally, the most important mineral phases must be selected according to the correct criterion that correlate this and the environment where could be formed.

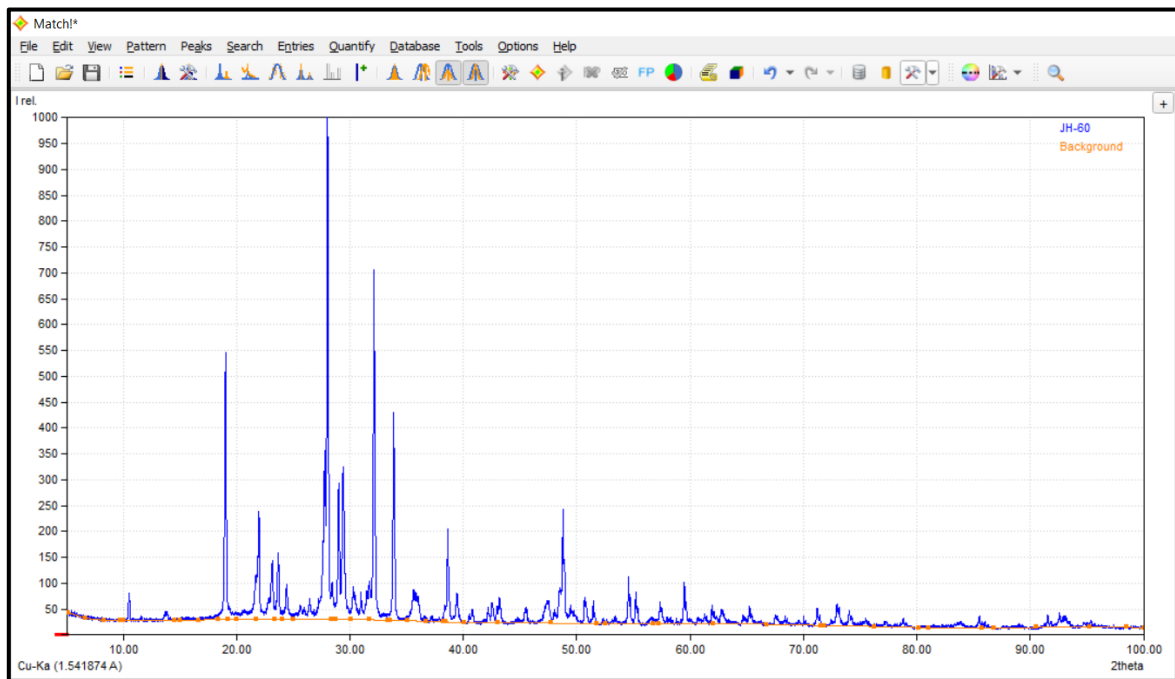


Figure 12. Interference Figure. The blue line represents the interference figure obtained as data from the XRD analyzer. This figure is processed by the software Match! To identify the different mineral phases present in the sample (Author).

7 Results

The following chapter presents the result of the deterioration problem associated with salt growing process in the architectural structures of Riobamba City. This chapter consist of three sections. The first one describes the deterioration process associated with salt growing process in the different kinds of architectural structures. Likewise, in this section is characterized the weathering process that takes place in these structures. The second section shows the results from the analyzes done over the aggregates employed in Riobamba. Finally, in the last section, the different mineral phases associated with the deterioration process are described.

7.1 Deterioration of Architectural structures

Based on the observations realized in the different field trips by the streets of Riobamba city was possible to verify that the deterioration problem associated with salt growing process is present in historical heritage buildings as well as republican buildings. However, the deterioration level in both structures is different. Likewise, this problem specially affects republican buildings.

In historical heritage buildings, the damage occurs in areas that have been restored or covered by modern mortars. According to the owners, in private buildings is normal to use modern mortars to repair or protect this type of structures. Since the municipality only forces the owners to maintain the architectural style without paying much attention to the materials used. The salt growing process produces the detachment of the mortar [Figure 13a) and c)]. This produces big holes in the walls exposing the historical heritage structure at the environment [Figure 13a)]. Figure 13b) shows that the deterioration process affects specially the mortar surrounding the volcanic rocks disposed of in the base of the structure. Likewise, in historical heritage public buildings, where it is trying to keep the original building materials. were given maintenance, due to no samples of salts found here.

In republican buildings, the deterioration problem corresponds to a cyclic process that manifest itself in the form of efflorescence and/or in form of alveolar erosion. This kind of deterioration represent an aesthetic problem, due to, the salts growing ruins the facades of the buildings. Likewise, this ruins the internal walls, associating with the buildings deteriorated and careless aspect, and forced the owners to spend money periodically.



Figure 13. Historical Heritage Buildings of Riobamba City. The figure shows three different kind of historical heritage buildings which were covered or fixed by modern mortar. In these three buildings the salt growing process is limited to the zones covered by modern mortars. The picture a) shows a big hole where the mortar has been removed exposing the rammed earth, inside the wall, to the environment. In the picture b) the deterioration is associated at the mortar surrounding the volcanic rocks arranged in the base of the wall. Finally, picture c) shows slat growing affection in the façade of the building (Author).

In white and gray buildings if this process is not deal with, produces the complete removal of the mortar that covers the bricks. Likewise, in dark work buildings, the salt growing produces the removal of material that joins the bricks within the wall. This can also happen in white and gray work buildings when the deterioration process is severe and extended in time.

The present research did not find evidence that slats growing put in immediately danger the structural integrity of buildings. It is because the damage caused by salt growing is principally associated with walls. In addition, salt growing requires a long period of time to produce enough damage to walls. The most several affectations are present in abandoned constructions, where the mortar that cover the walls has been removed. According to the observations, only in these several cases of salt growing, the concrete that covers iron rods has been removed exposing the iron rods to the environment (Figure 14). When the iron rods are exposed to the environment, they tend to be weathering in the form of corrosion.

The corrosion in iron metals is the result of action to hydrated oxides that increasing the iron original volume. In general iron materials are dep in structures as a consequence its interaction with water is restricted. However, in case both stay in contact, the stress produced by the iron expansion is enough to produce cracks in the surrounding material (Torraca, 2005) (Figure 14).



Figure 14. Several Cases of Salt Growing. The figure shows a several cases of slat growing where the mortar that cover the walls and the concrete that covers the iron rods have been removed. Likewise, the iron rods exposed in the lower part of the column show signs of oxidation. Even though the iron rods are exposed, no flexion of the concrete column is seen (Author).

Due to the size of the city, the neighborhood known as El Retamal was taken as a sample zone. The total structure in this zone corresponds to republican buildings. The data shows that the deterioration process especially affects white work buildings (79%), followed by gray work buildings (15%) and finally dark works (6%). Likewise, the data shows the affinity between the salt growing process with the building material. From the 72 samples taken in El Retamal, 94% of samples were taken in plaster mortars, 4% in mortars employed to join bricks and the last 2% corresponds to salts that growing in bricks (1% terracotta, 1% concrete) (Figure 15). The total data from this zone is shown in Annex 4.

From the observations the level of deterioration associated with salt growing is intermedium because this only affects the aesthetic appearance of the buildings. This forces to owners to spend money to repair and/or maintain the good facades aspect of their homes. Fortunately, this phenomenon does not represent a structural problem for the structures.

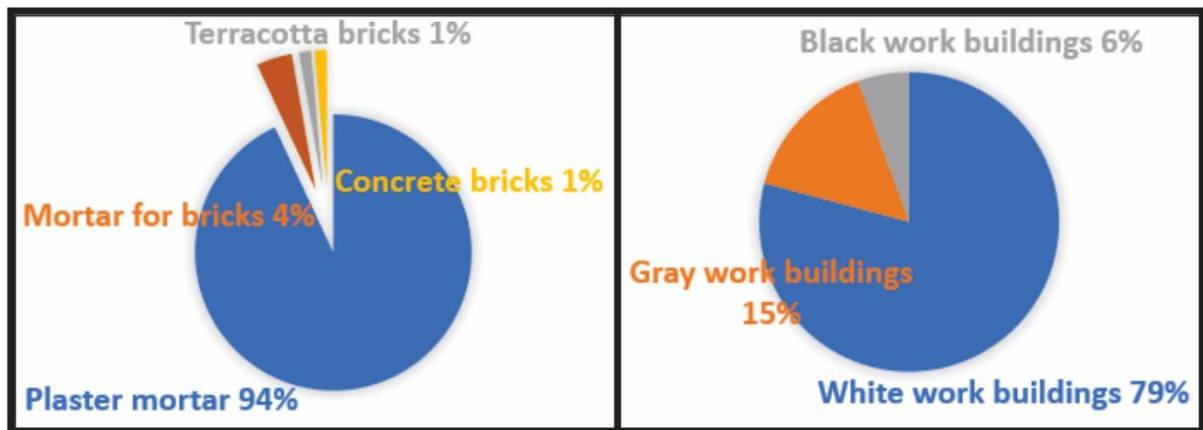


Figure 15. Salt Growing Incidence in Republican Buildings. The left figure shows the relationship between the salt growing phenomenon with the different mortars and bricks employed in civil architecture. The right figure shows the incidence of salt growing according the three kinds of republican building (Author).

Characterization of the Deterioration Process.

The deterioration process that affects the architectural structures in Riobamba city is the result of two natural phenomena that consist in efflorescence and alveolar erosion.

Efflorescence is the salt crystallization process that takes place inside pores. These pores are specially located in the surface of the material, where the disruptive effect is smaller. This process is driven by high temperatures and low-speed winds. Efflorescence forms big cumulus of salts upon the mortars (Torraca, 2005).

Alveolar erosion corresponds to a desegregation process forming deep cavities or alveolus by the action of the salt crystallization process. At high temperatures the evaporation rate on the surface is higher than inside, as a result, the surface turns dry while anhydrous is formed inside. The pressure from anhydrous salt is enough to disaggregate the dry surface. In addition, the disaggregate process is accelerated by the action of wind (Torraca, 2005).

In both cases, the nucleation occurs inside of the micropores present in the most external zone of the wall. However, Alveolar erosion represents the biggest problem because produces the continuous disintegration of mortars. The affectation caused by salt growing manifests itself as a salt cumulus of white color. The way how salts cumulus is arranged is varied. Most of salts are present in form of white lines that could extended by many meters or a few centimeters [Figure 14(A, B, E)]. Nevertheless, other salts stay in the forms of sub-angular cumulates (Figure 14B). Likewise, these in general stay present in the walls of the ground floor, in zones close to the sidewalk. However, many of them manifest on the first floor, or terraces (Figure

14A). In most cases, the salts are present in zones of the walls that show humidity, but it is not always fulfilled (Figure 14D). In addition, the deterioration associated to salts growing not only affects facades, this also affects the internal walls of the buildings (Figure 14F). The Figure 16 shows in general how this phenomenon is widely distributed around the city.

Haynes (2002) determines that the damage associated with salts is the result of the following process: crystallization of salts from supersaturated solution, and changes in the hydration state of the salt. Both processes take in place inside the pores present in the material. When crystals fill up the pores, these eject pressure over the walls. The pressure produced by salts is capable to break the pores (Torraca, 2005). In architectural structures the damage by salt crystallization is associated with many groups of salts (Doehne, 2002).

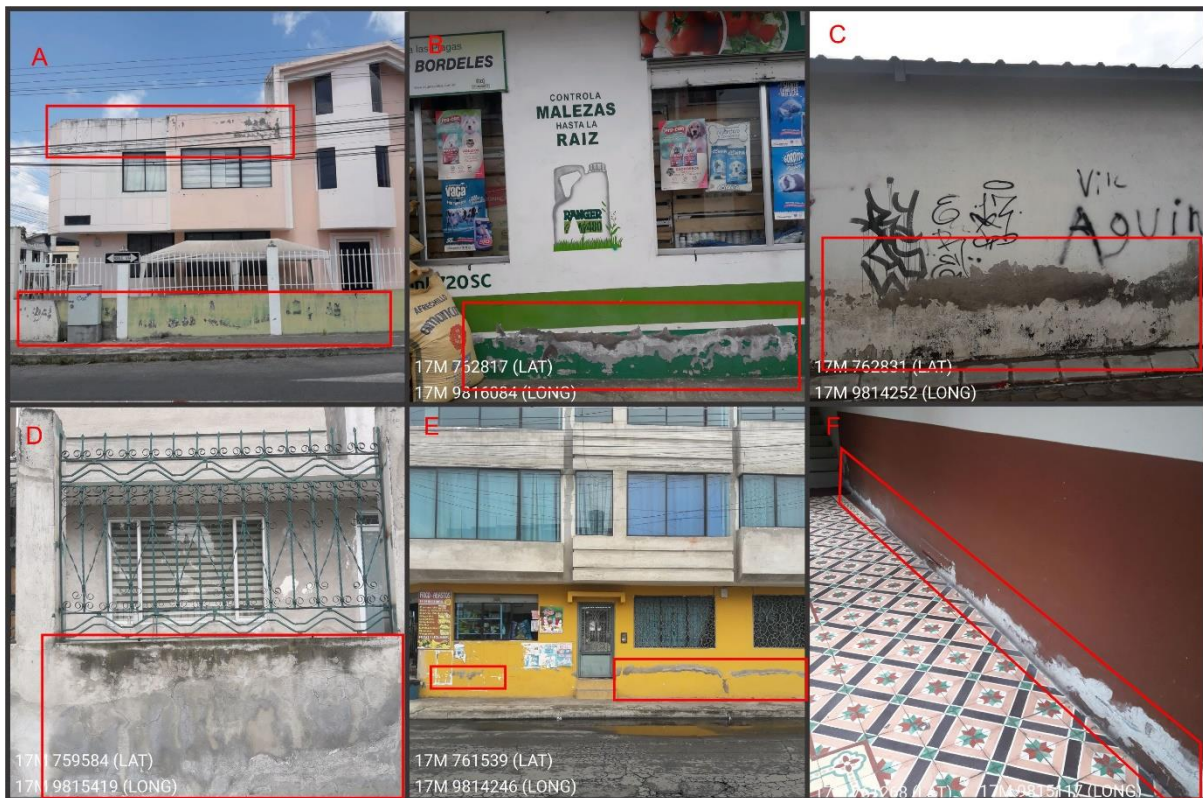


Figure 16.. Distribution of the Problematic around the Riobamba city. This figure represents six different republican buildings located in different parts of the city where the salt growing deterioration is present especially in façades, but it is also inside the buildings. The pictures A, B, C, and the ground floor of picture E represent white work buildings affected by salt growing producing the deterioration of the facades. Picture D shows how salt growing process affects gray work buildings. Finally, F shows that salt growing also occurs in the internal walls of the buildings (Author).

7.2 Building Materials Analyses

As was enunciated previously, the materials employed in republican buildings corresponds to cement, iron hoods, bricks, and aggregates. From these materials, cement, iron rods, terracotta, and concrete bricks, come from different parts of Ecuador. Only aggregates

come from Riobamba City. Aggregates corresponds to sands and stones, these are mined from the nearby quarries (Figure 2).

The following section describes in detail the different aggregates mined in the city. The description begins with the precedence of the material (quarries) and ends by showing the data about the different analyses done over each kind of aggregate.

Quarries

In response to the Solicited letter delivered by the author of this project, on March 05 of 2021, the municipality of Riobamba city sends in the same month the response Nro 383975 (Annex 5). This document certifies the following information: The municipality of Riobamba city assumed control of the different quarries in 2014. In the municipality are registered 42 quarries from them only 6 still working. However, in the different field trips was verified that only 5 quarries still working (Figure 2). The material is obtained from an open pit mining way where is only employed heavy machinery avoiding the use of explosives.

The material that is currently mined come from the Riobamba Unit (R-DAD). These quarries are in the east, northwest, and west of the city (Figure 2). Likewise, it is important to mention that Mira flores quarry located in the northwest of the city belongs to the municipality of Guano. But because its importance to the Riobamba city, the present study takes into count this quarry (Figure 2).

Geology of the Quarries

The five quarries that still working in the city mined the material from the Riobamba Unit (R-DAD). The R-DAD was described first by Lozada in 1976, as a lahar deposit. Posteriorly, Clapperton in 1990 describes this as a debris avalanche deposit (DAD) in base of its morphology characteristics. Recent studies, such as Barba et al. (2008) and Samaniego et al. (2012), accept the classification as a DAD.

Bernard et al. (2008), describes the quarries located at the east as volcano-sedimentary deposits which reach a thickness of up to 100 m. The deposit consists of a volcanic breccia composed of two sedimentary facies the mixed facies (Mf) and block facies (Bf) (Figure 17).

How the R-DAD is a debris avalanche deposit, the distribution of the different facies respects each other varies in the quarries. Figure 17 shows how the Bf overlies the Mf. The

deposit reaches a high of 50 m. The Mf deposited in the bottom shows light colors, and reaches an approximate high of 40 m. The Bf shows dark colors and reaches an approximate high of 10 m. In the top is deposited a paleo-soil of yellow color.

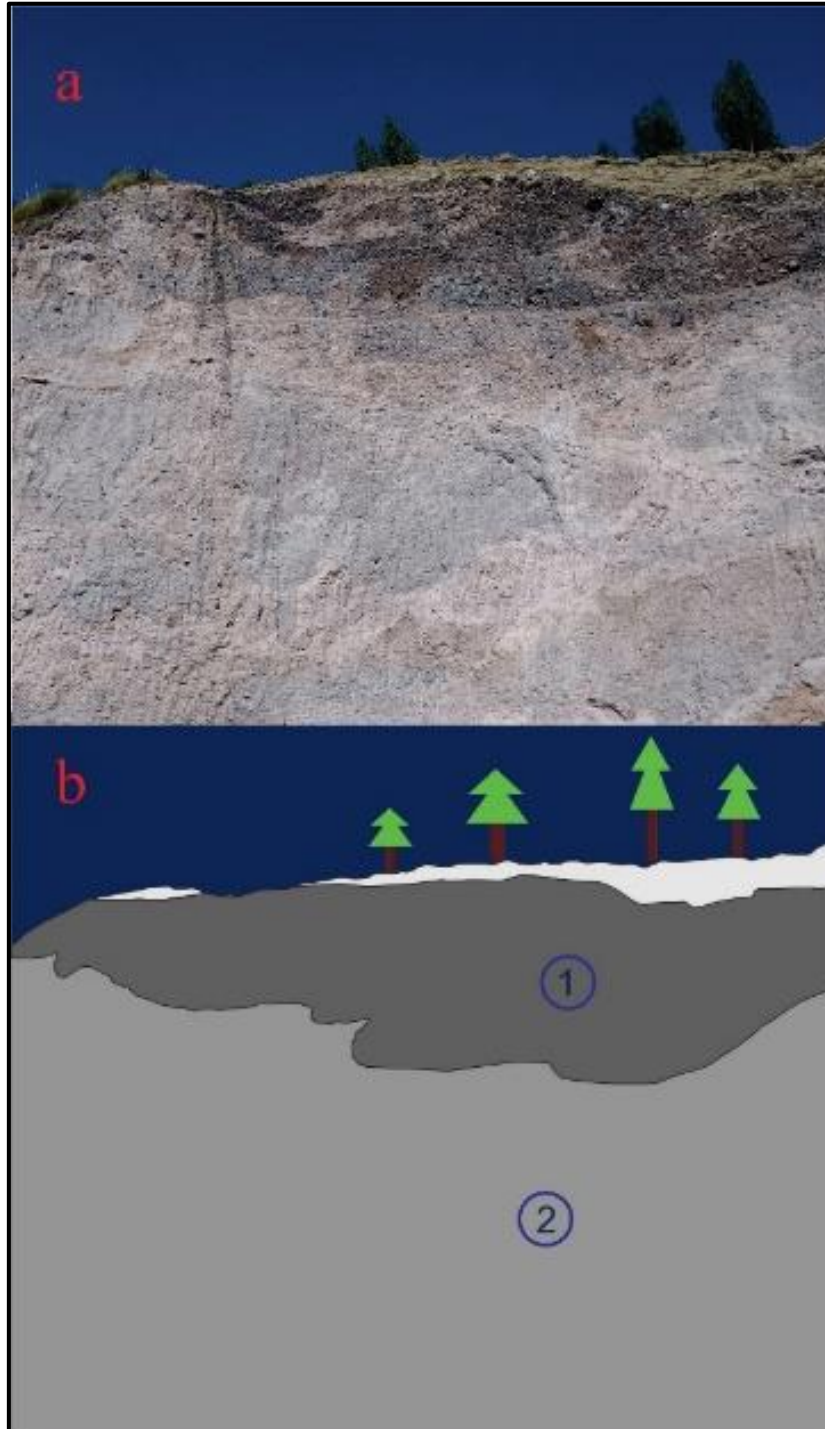


Figure 17. Spatial Distribution of the Facies that Conforms the R-DAD. This corresponds mined slope from the Sillahuan quarry locates at the west of the city. The deposit reaches up 50 m. This is composed of two facies, the Mf (2) in the bottom with the Bf (1) over this. The Mf shows light colors corresponding a matrix supported massive deposit. On the other hand, the Bf show more dark colors, although this is a matrix supported deposit too, here it is possible to appreciate clasts of different size (Author).

Mixed Facies (Mf)

The mixed facies (Mf) consist of many volcanic lithologies randomly contained in a silty-sandy matrix (Figure 18). Barba (2016) classify the rocks into amphibole andesites and two-pyroxenes andesites. There is not data about the age of this deposit. However, it is considered older than 68 ka. This estimation is in base of the age dated from a volcanic deposit that overlays the R-DAD (Samaniego et al., 2012).

In the quarries the mixed facie consists of deposits of light colors which reach a thickness of up to 40 m (Figure 18). However, the distribution of this facie varies in each quarry and sometimes it is impossible to distinguish between the Mf and Bf. This is a massive deposit that presents many colors such as: yellow, beige, red and gray. It is matrix-supported, and poorly sorted. The matrix is composed of silty to fine sand. The clasts are sub-angular, their sizes vary from 10 to 25 cm, and parents low sphericity. It is common to find diaclosed bombs, these bombs are gray color, sub angular, around 1 m size (Figure 18). Finally, some deposits show the presence of pipes. These pipes reach a thickness of up to 4 m, and are yellow color, matrix-supported, and poorly sorted. The matrix is composed of silty yellow material. The clasts are gray and sub-angular of 5 to 15 mm.

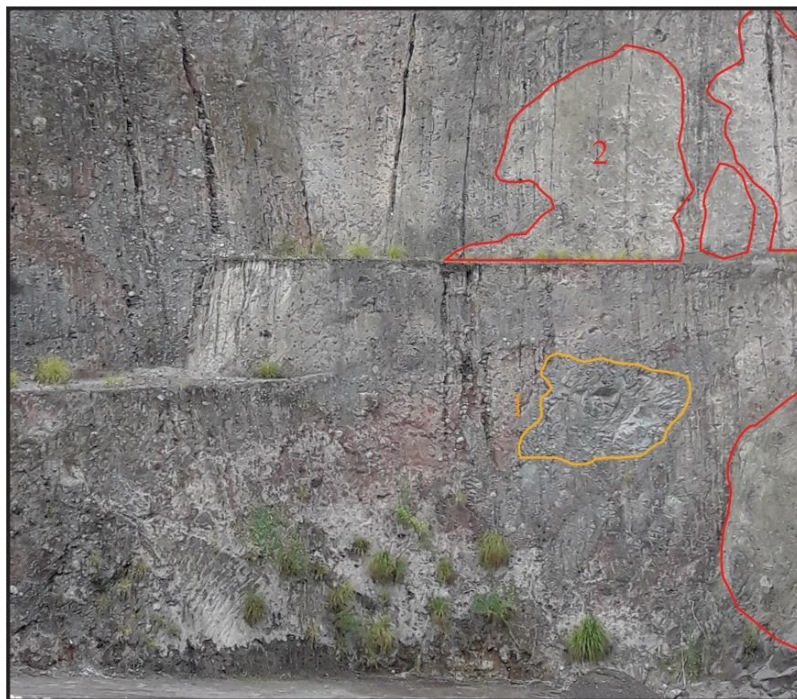


Figure 18. Mixed Facies Mf. The Mf shown in the figure belongs to a mined slope from the Mira Flores quarry located in the north of the city. Here the Mf reaches up 22 m. Inside this deposit is contained diaclosed rocks of around 1.5 m in size (1). Likewise, it is possible to distinguish some intrusions that correspond to yellow pipes. These pipes reach up to 3 m of thickens (2) (Author).

Block Facies (Bf)

The block facie according to Clapperton (1990), consists in a clast supported deposit. The different clasts contained inside here corresponds to pyroxene andesites, and basic andesites, in addition, some clasts show red colors sign of hydrothermal alterations. The matrix is composed of pulverized fragments coming from the big clast surrounding. The date for this facie is estimated the same as the Mf (Samaniego et al., 2012).

In many quarries, the block facie is distributed randomly and is difficult to distinguish. However, in this quarry, the Bf is in the upper part and reaches up to 8 m. The deposit is gray color, massive, matrix-supported, and poorly sorted. The matrix is composed of light brown material of fine to medium grain size. The clasts correspond to andesites whose size varies from 3 to 45 cm. These are gray in color, angular, and low-sphericity. Some clast shows red color (Figure 19).



Figure 19. Block Facies Bf. The Bf shown in the figure belongs to a mined slope from the Cerro Negro quarry located in the east of the city. Here the Mf reaches up to 22 m. this consist of a matrix-supported massive deposit poorly sorted. The clast size varies from 3 to 45 cm (Author).

Way of Mining and Aggregates Expended

The way of mining corresponds to an Open-pit mine, where the material is removed employing heavy equipment forming terraces [Figure 19(a)]. Posteriorly, this material is transport in dump trucks toward the zones where will be processed. And finally, the material is classified to obtain the different kinds of aggregates to be commercialized.

In bigger quarries, the process of classification corresponds to a series of sieves that separate the material according to the grain size. The first sieve separates any clast bigger than 51 mm. After the first classification the material less than 51 mm is sieved again to separate the gravel mixed in the sand. And finally, the sand is sieved through a sieve of 200 to obtain the material that is expended as fine sand [Figure 19(b)].

The rest of the material is classified in medium to coarse sands and gravel (ripio, spell). On the other hand, the material bigger than 51 mm is shredded to obtain clasts of grain size less than or equal to 51 mm [Figure 19(c)], in concordance with the specifications designed in the NTE (2011). The shredded material is sieved to obtain medium to coarse sands and gravel. Posteriorly, these are added to the material that was sieved first maintaining the classification of medium to coarse sand and gravel. In many cases the shredded sand is not mixed with the sieved sand and is sold separately. On the other hand, in little quarries the material is classified only employing sieves, and maintaining the same classification described previously.

From the previous explanation, the aggregates expended by the quarries are classified into the three following groups: sieved sand (fine sand), shredded sand (medium to coarse sand), and ripio (spell, 51 mm). The information about different aggregates expended in each quarry is presented in Table 2.

Table 2. Kind of Aggregates marketed in each one of the quarries visited by the author.

Quarry	Material					
	Sieve sand		Sieve ripio	Shredded sand		Shredded ripio
	Fine	Medium to Coarse		Fine	Medium to Coarse	
Cerro Negro	X	X	X	-	X	X
El Cisne	X	X	X	-	-	-
Mira Flores	X	X	X	-	-	-
La Ponderosa	X	X	X	-	-	-
Sillahuan	X	X	X	-	X	X

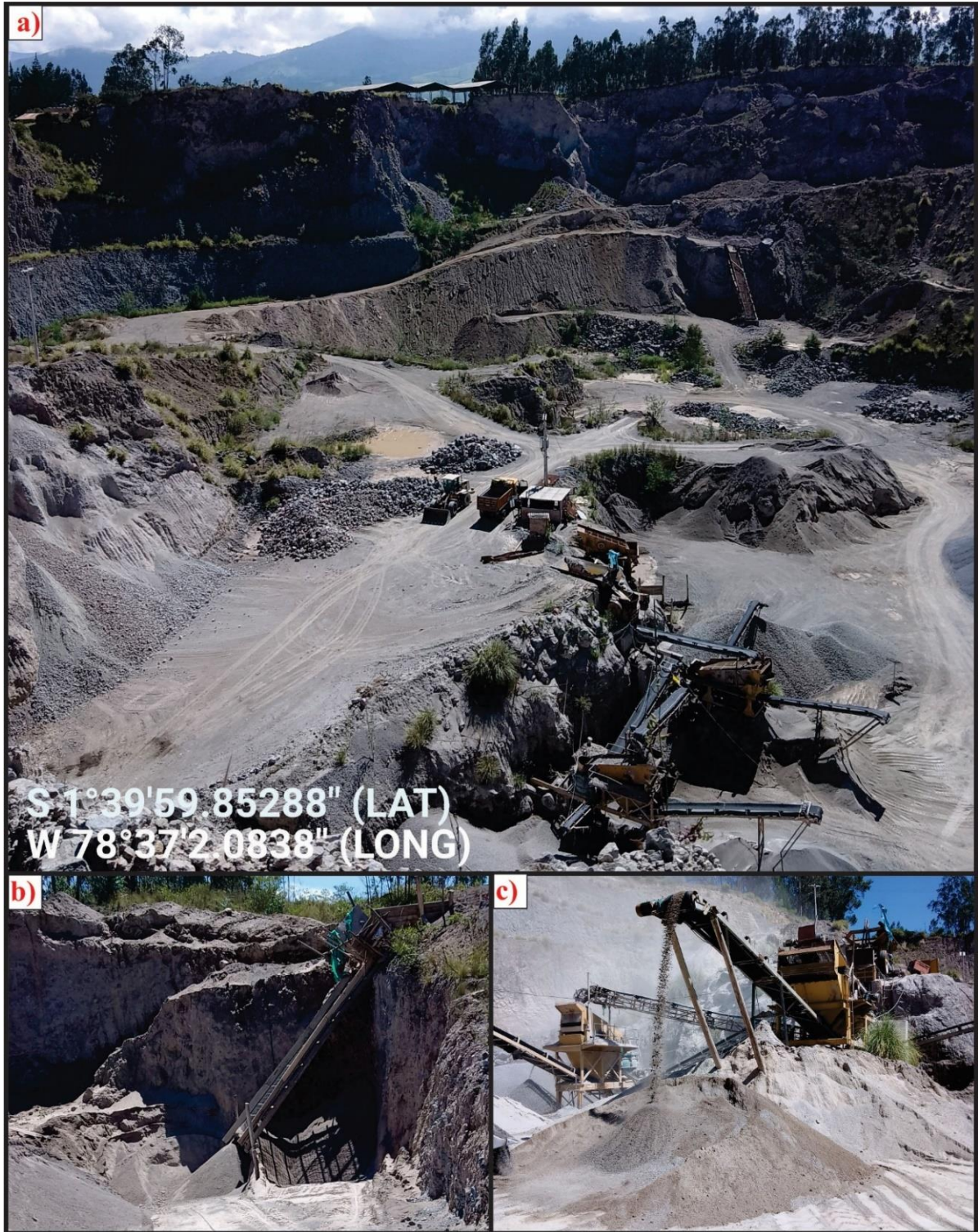


Figure 20. Cerro Negro Quarry. This corresponds to one of the oldest quarries in the city. The figure is composed of three pictures that show the mining process. image (a) shows a typical quarry in the city where the material is mined employing heavy machinery forming terraces. e image (b) shows a sieve employed to separate the sand and stones from the material mined. image (c) shows a shredder employed to reduce big clasts into smaller rocks known as ripio (Author).

Fine sand or Sieve sand: This sand is composed of 90% fine sand and a 10% of lithics. The fine sand is of light-beige color. Which is composed especially of glassy crystals and, in minor proportion, black and brown particles. The mineral composition corresponds to plagioclase, amphibole, pyroxene, and quartz. The lithics size is below 3 mm. These are of gray and black color, angular, with medium sphericity (Figure 21).

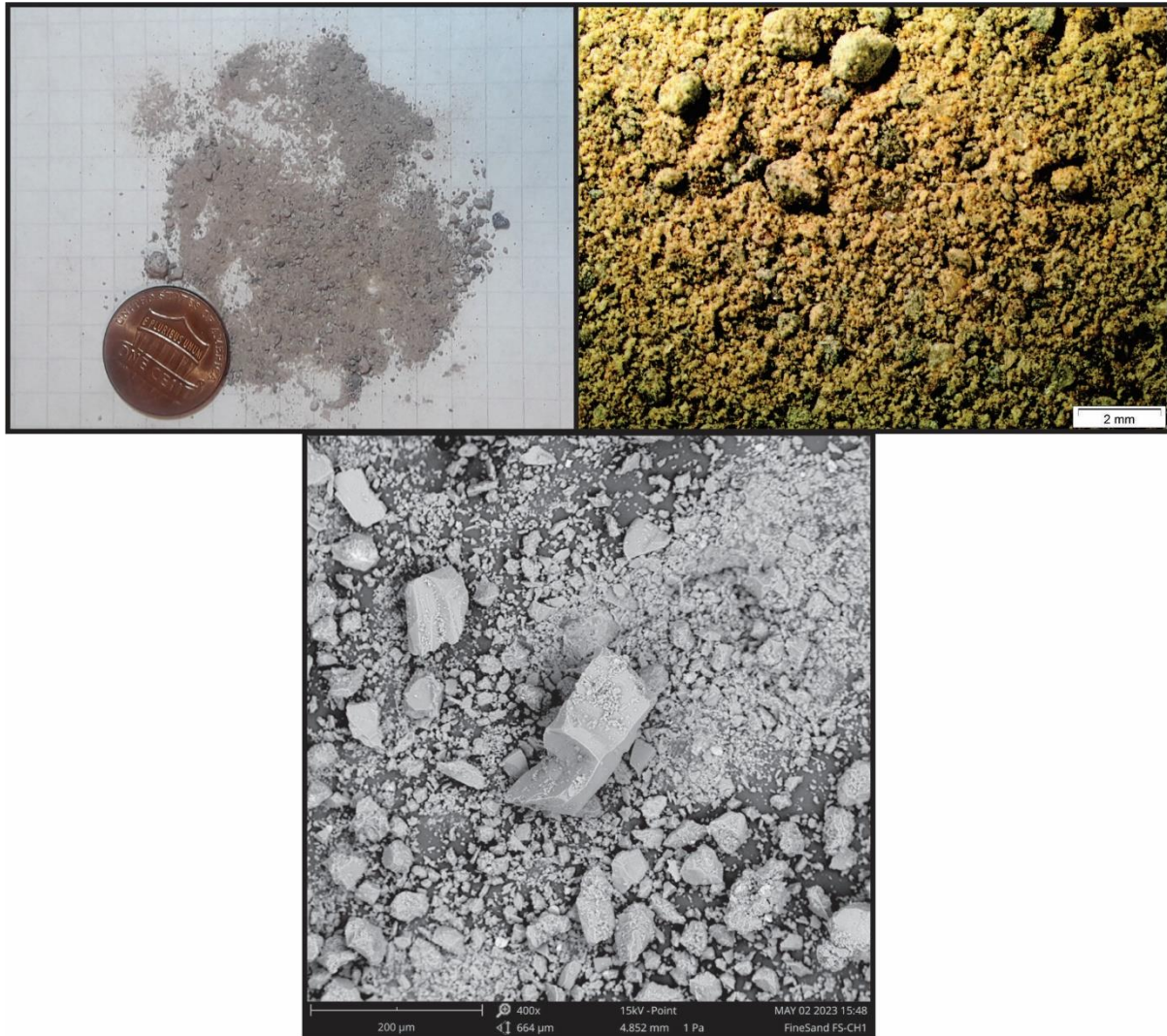


Figure 21. Fine Sand for Plastering mortars. The fine sand marketed independently of the quarry comes from a sifting process. Fine sand is composed of 90% fine sand and a 10% of lithics. The different pictures show the same sand under different levels of zoom amplification (Author).

The sieved sand is employed in plaster mortar. This kind of mortar is employed to plaster walls. According to civil engineer Israel Criollo the correct dosage corresponds to three to four parts of sand with one part of cement and water. The volume of water is according to the brand of cement. All these materials are mixed until a dense gray paste is obtained. This paste is smeared upon walls, ceiling, and columns until it forms a layer 2 cm thick.

Medium to Coarse sand: This sand is composed of 80% medium sandgrain size and a 20% of lithics. The sand is of light-gray color, composed of glassy crystals mixed with black and brown particles. The mineral composition corresponds to plagioclase, amphibole, pyroxene and quartz. The lithics corresponds to andesites, dacites and tuffs, which size varies from 2 to 10 mm (Figure 22). These are angular, with low sphericity many of them are planar. Some clasts present fractures this could be the result of the shredded process.

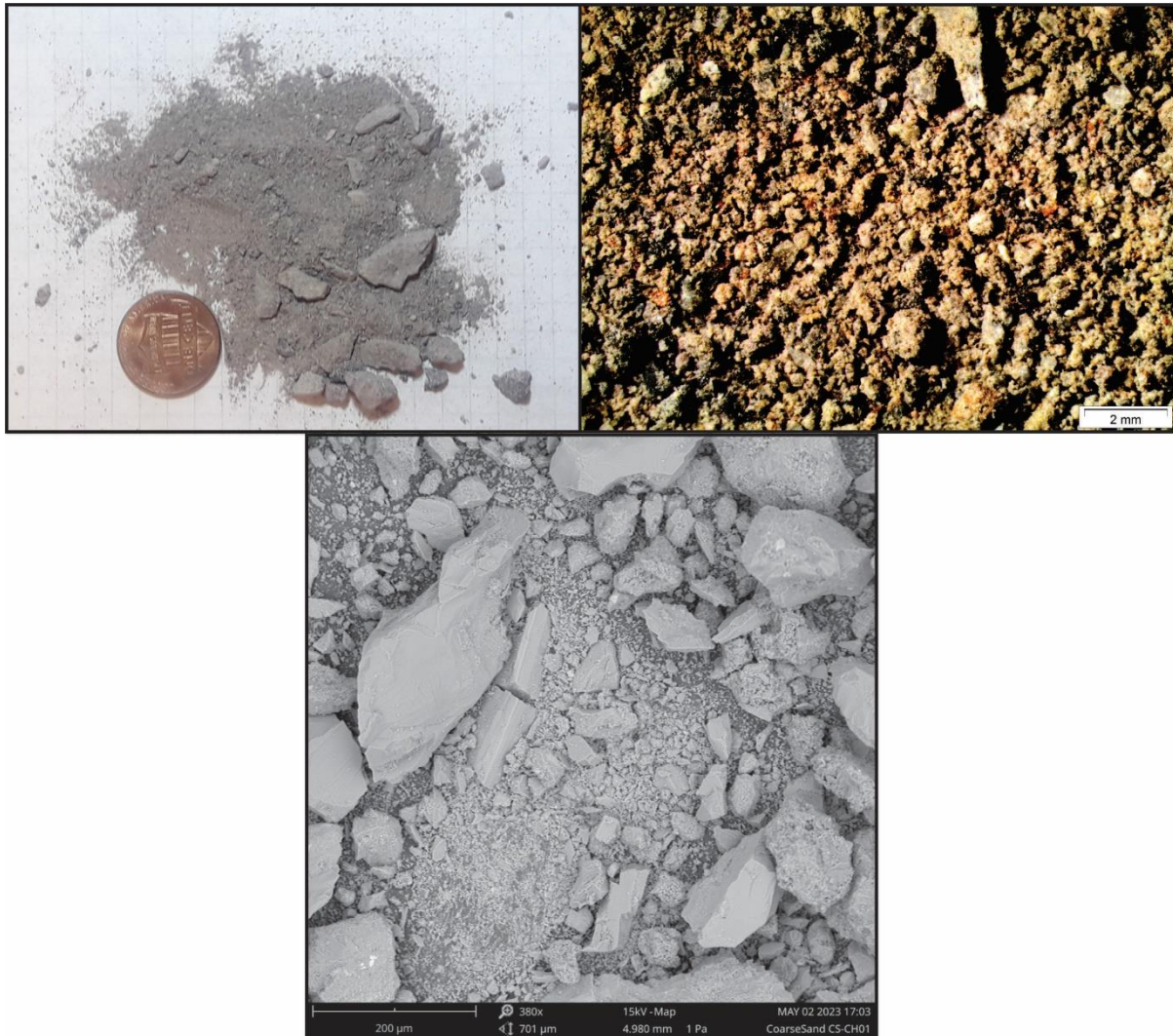


Figure 22. Medium to Coarse Sand. This kind of sand is employed for mortars to join bricks. This sand is composed of 80% medium sand grain size and 20% of lithics. This kind of sand comes in two different ways. The first corresponds to a sifting process and the second is a shredded process. The figure shows shredded sand, taken from Mira Flores quarry, under different levels of zoom amplification (Author).

The shredded sand is employed in mortars used to join bricks to build walls. According to civil engineer Israel Criollo the correct dosage corresponds to two to three parts of sand with one part of cement and water. The volume of water is according to the brand of cement. All these materials are mixed until a dense gray paste is obtained. This paste is smeared between

bricks to join one with the other. In addition, this mortar is employed to join the walls at the columns.

Ripio (spell): This consists of a mixture of volcanic rocks whose size varies from 10 to 51 mm. The form of the rocks varies from angular of low sphericity to sub-angular of medium sphericity. The volcanic rocks correspond to: andesites, amphibole andesites, amphibole-pyroxene andesites, amphibole-plagioclase andesites. (Figure 23 and Annex 3).

Ripio in addition to shredded sand, cement, and water are mixed to produce concrete. Concrete is employed to build columns and slabs. This mixture is in direct contact with iron rods. Both materials, concrete and iron rods, are responsible for the structural stability of the building.



Figure 23. Ripio. Is known as Ripio at the mixture of rocks composed of: andesites, amphibole andesites, amphibole-pyroxene andesites, amphibole-plagioclase andesites and, tuffs, expended as aggregate by the concrete to produce concrete, employed in slabs and columns. To be considered as Ripio the size of rocks must be between 10 to 51 mm (Author).

Chemical Analysis of the R-DAD and the Aggregates

The first study to determine the chemical composition of Chimborazo volcano was carried out by Killian (1987). This study consisted of the X-RF and Electron Micro-probe analysis to determine the major elements present in the different lithologies. The present research only was taken in the count which lithologies deposited at the SSE from Chimborazo Volcano and correspond to the R-DAD. The lithologies defined by Killian correspond to the following: 1) The Riobamba Formation (R-DAD) blast to SSE, posteriorly defined as the R-DAD by Clapperton (1990); 2) Juvenile magma within RBF, which according to its characteristics corresponds to the pipes inside the R-DAD (Figure 17); 3) The major element composition of this lithologies is described in the three first position of Table 3 respectively. Posteriorly, in 2016, Barba analyzed samples from the R-DAD located to the east of Riobamba in the Riobamba-Penipe highway obtaining the results described with the code CH DB 33 (A-G) showed the lower part of Table 3.

Table 3. Chemical composition of samples associated with R-DAD taken from the works of Barba (2016) and Clapperton (1990).

Sample	SiO ₂	TiO ₂	Al ₂ O ₃	Fe ₂ O ₃	MnO	MgO	CaO	Na ₂ O	K ₂ O	P ₂ O ₅
1)	75,2	0,19	12,86	1,12	0,04	0,26	1,38	3,65	2,84	0,06
2)	65,03	0,61	18,22	1,13	0,09	1,81	4,88	3,12	1,06	0,7
3)	60	0,75	17,06	6,2	0,09	3,55	5,8	4,18	1,63	0,22
CH DB 33A	61,07	0,68	17,43	6,05	0,09	2,84	5,81	4,44	1,38	0,21
CH DB 33B	62,15	0,74	16,98	6,11	0,07	2,23	5,41	4,52	1,57	0,23
CH DB 33C	62,28	0,58	16,43	5,84	0,09	2,75	5,68	4,19	1,88	0,29
CH DB 33D	60,84	0,75	17,27	6,38	0,1	2,82	5,96	4,25	1,42	0,21
CH BD 33E	60,94	0,7	17,51	6,02	0,09	2,75	6,05	4,26	1,47	0,2
CH DB 33F	59,41	0,83	17,24	7,03	0,1	3,29	6,44	3,97	1,47	0,22
CH BD 33G	56,79	0,97	15,5	7,34	0,1	3,63	7,67	3,89	3,4	0,71

To complement this information, in this study was done the chemical analysis of the two kinds of sands expended by the quarries. These sands were taken from Cerro negro quarry. How was explained previously. The sands according to their precedence correspond to: sieve fine sands (Table 4) and shredded sands (Table 5). The total number of sand samples could not be analyzed due to equipment breakdown.

Table 4. Chemical composition of the sieved sand sold as fine sand from the Cerro Negro quarry. Fine sand mixed with water and cement form the mortars that will be employed in the endings of the building (facades, and to cover walls columns, and roofs).

Element name	Atomic number	Element symbol	Atomic concentration percentage	Weight concentration percentage
Oxygen	8	O	67.76	53.09
Silicon	14	Si	16.40	22.56
Aluminum	13	Al	7.18	9.49
Iron	26	Fe	1.46	3.99
Sodium	11	Na	3.34	3.76
Calcium	20	Ca	1.68	3.30
Magnesium	12	Mg	1.28	1.52
Potassium	19	K	0.41	0.78
Indium	49	In	0.06	0.35
Sulfur	16	S	0.20	0.35
Titanium	22	Ti	0.10	0.23
Manganese	25	Mn	0.03	0.08
Chromium	24	Cr	0.02	0.06

Table 5. Chemical composition of the shredded sand sold as medium to coarse sand from the Cerro Negro quarry. Medium to coarse sand mixed with water and cement form the mortars employed to join bricks to build walls. In addition, Medium to coarse sand mixed with water, ripio and cement produce concrete.

Element name	Atomic number	Element symbol	Atomic concentration percentage	Weight concentration percentage
Oxygen	8	O	68.62	54.42
Silicon	14	Si	17.10	23.80
Aluminum	13	Al	6.70	8.96
Sodium	11	Na	3.49	3.97
Calcium	20	Ca	1.53	3.04
Iron	26	Fe	0.94	2.60
Potassium	19	K	0.60	1.17
Magnesium	12	Mg	0.78	0.94
Tellurium	52	Te	0.14	0.87
Titanium	22	Ti	0.10	0.23

7.3 Mineral Phases Responsible of the Deterioration of Architectural structures

To determine the different mineral phases was necessary to do an X-RD analysis (Figure 12). In base of the results, the mineral phases acting in the city in order of abundance correspond to thenardite, albite, calcite, anorthite, magnesium calcite, and nitratine presented in the Figure 24 a). From these minerals, albite and anorthite corresponds to plagioclase remnant from the sand used in the mortar preparation.

The rest of the mineral phases correspond to salts that the bibliography design as responsible for the deterioration process of architectural structures. In base the chemical composition of the different salts found in the architectural structures of the city corresponds to: sulfates (thenardite), carbonates (calcite, magnesium calcite), and nitrates (nitratine) how is showed in the Figure 24 b).

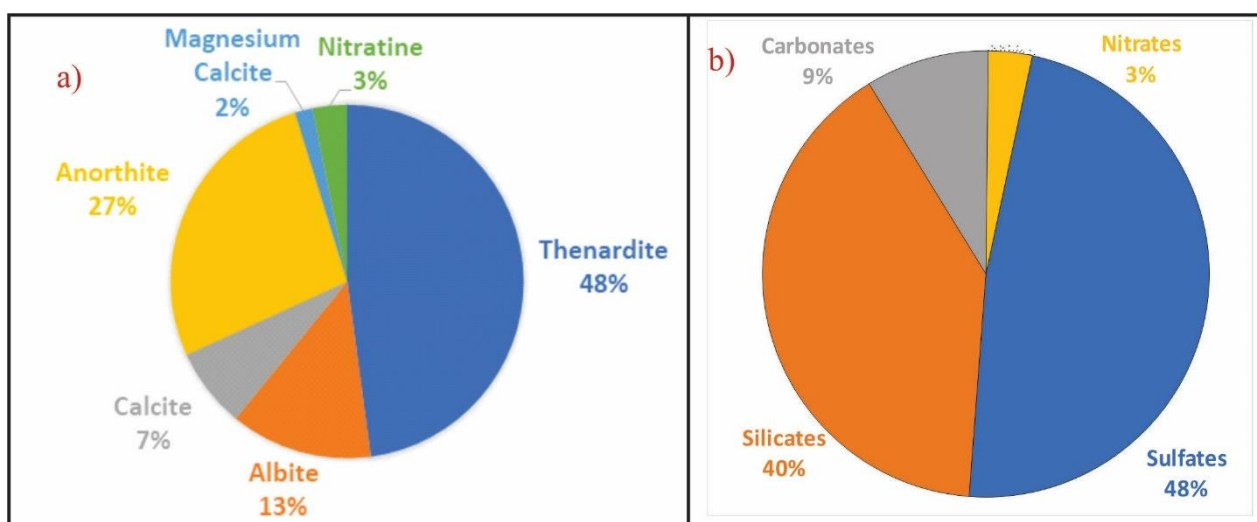


Figure 24. Percentage Distribution of the Different Mineral Phases Responsible in the Deterioration Process. This figure is composed of two graphics that represents the percentage distribution of the different mineral phases and salts responsible for the deterioration process in architectural structures of Riobamba city. The part a) represents the mineral phases and the part b) the salts species. Both graphs summarized the data exposed in Table 6, where the results from XRD are shown (Author).

Table 6. XRD results: The table shows the different phase minerals responsible for the deterioration process of the architectural structures in Riobamba city. To obtain these minerals was necessary to apply XRD analysis over these samples. This table, in addition to the mineral phases, also shows the formula, the crystal system, and the percentage of the mineral respect to the whole sample.

Sample	Building Kind	Coordinates		Mineral Phase	Formula	Crystal System	%
		Latitude	Longitude				
JH-01	Gray Building	-1,6495981	-78,6725649	Thenardite	Na ₂ SO ₄	Orthorhombic	0,356
				Albite	(Na,Ca)Al(Si,Al) ₃ O ₈	Triclinic	0,574
				Calcite	Ca(CO ₃)	Rhombohedral	0,069
JH-02	White Building	-1,6500939	-78,6726614	Thenardite	Na ₂ SO ₄	Orthorhombic	0,614
				Albite	(Na,Ca)Al(Si,Al) ₃ O ₈	Triclinic	0,328
				Calcite	Ca(CO ₃)	Rhombohedral	0,058
JH-05	White Building	-1,6515477	-78,6716774	Thenardite	Na ₂ SO ₄	Orthorhombic	0,66
				Albite	(Na,Ca)Al(Si,Al) ₃ O ₈	Triclinic	0,234
				Calcite	Ca(CO ₃)	Rhombohedral	0,105
JH-06	Gray Building	-1,6516896	-78,6716012	Thenardite	Na ₂ SO ₄	Orthorhombic	0,293
				Albite	(Na,Ca)Al(Si,Al) ₃ O ₈	Triclinic	0,63
				Calcite	Ca(CO ₃)	Rhombohedral	0,078
JH-09	Gray Building	-1,652369	-78,6710685	Thenardite	Na ₂ SO ₄	Orthorhombic	0,172
				Albite	(Na,Ca)Al(Si,Al) ₃ O ₈	Triclinic	0,374
				Calcite	Ca(CO ₃)	Rhombohedral	0,067
JH-11	Gray Building	-1,6526985	-78,6708832	Thenardite	Na ₂ SO ₄	Orthorhombic	0,17
				Anorthite	(Ca,Na)(Si,Al) ₄ O ₈	Triclinic	0,835
JH-15	White Building	-1,6542245	-78,6700822	Thenardite	Na ₂ SO ₄	Orthorhombic	0,447
				Anorthite	(Ca,Na)(Si,Al) ₄ O ₈	Triclinic	0,368
				Magnesium Calcite	(Mg _{0,03} , Ca _{0,97})(CO ₃)	Rhombohedral	0,186

Sample	Building Kind	Coordinates		Mineral Phase	Formula	Crystal System	%
		Latitude	Longitude				
JH-18	White Building	-1,6564706	-78,6689984	Thenardite	Na ₂ SO ₄	Orthorhombic	52,30%
				Anorthite	(Ca,Na)(Si,Al) ₄ O ₈	Triclinic	47,70%
JH-20	White Building	-1,6571453	-78,668801	Thenardite	Na ₂ SO ₄	Orthorhombic	44,30%
				Calcite	Ca(CO ₃)	Rhombohedral	55,70%
JH-23	White Building	-1,6565556	-78,6708722	Thenardite	Na ₂ SO ₄	Orthorhombic	31,30%
				Anorthite	(Ca,Na)(Si,Al) ₄ O ₈	Triclinic	65,80%
				Calcite	Ca(CO ₃)	Rhombohedral	2,90%
JH-26	White Building	-1,6594848	-78,6660781	Thenardite	Na ₂ SO ₄	Orthorhombic	21,90%
				Anorthite	(Ca,Na)(Si,Al) ₄ O ₈	Triclinic	73,30%
				Calcite	Ca(CO ₃)	Rhombohedral	4,80%
JH-28	White Building	-1,6497309	-78,6719304	Thenardite	Na ₂ SO ₄	Orthorhombic	21,10%
				Anorthite	(Ca,Na)(Si,Al) ₄ O ₈	Triclinic	78,90%
JH-31	White Building	-1,6509631	-78,6711161	Thenardite	Na ₂ SO ₄	Orthorhombic	75,50%
				Calcite	Ca(CO ₃)	Rhombohedral	24,50%
JH-32	White Building	-1,6522786	-78,6698895	Thenardite	Na ₂ SO ₄	Orthorhombic	18%
				Anorthite	(Ca,Na)(Si,Al) ₄ O ₈	Triclinic	74,10%
				Calcite	Ca(CO ₃)	Rhombohedral	7,90%
JH-33	White Building	-1,6526296	-78,6697286	Thenardite	Na ₂ SO ₄	Orthorhombic	26,60%
				Anorthite	(Ca,Na)(Si,Al) ₄ O ₈	Triclinic	44,40%
				Calcite	Ca(CO ₃)	Rhombohedral	29%
JH-35	White Building	-1,6540058	-78,6686597	Thenardite	Na ₂ SO ₄	Orthorhombic	48,70%
				Anorthite	(Ca,Na)(Si,Al) ₄ O ₈	Triclinic	48,60%
				Calcite	Ca(CO ₃)	Rhombohedral	2,70%
JH-36	White Building	-1,6545076	-78,6679952	Thenardite	Na ₂ SO ₄	Orthorhombic	65,80%
				Albite	(Na,Ca)Al(Si,Al) ₃ O ₈	Triclinic	25,40%
				Calcite	Ca(CO ₃)	Rhombohedral	8,80%
JH-38	White Building	-1,6552621	-78,6671514	Thenardite	Na ₂ SO ₄	Orthorhombic	66,20%
				Anorthite	(Ca,Na)(Si,Al) ₄ O ₈	Triclinic	28,60%
				Calcite	Ca(CO ₃)	Rhombohedral	5,20%

Sample	Building Kind	Coordinates		Mineral Phase	Formula	Crystal System	%
		Latitude	Longitude				
JH-41	White Building	-1,6557993	-78,6665724	Thenardite	Na ₂ SO ₄	Orthorhombic	71,70%
				Albite	(Na,Ca)Al(Si,Al) ₃ O ₈	Triclinic	23,90%
				Calcite	Ca(CO ₃)	Rhombohedral	4,50%
JH-42	White Building	-1,6560308	-78,666307	Thenardite	Na ₂ SO ₄	Orthorhombic	45,90%
				Anorthite	(Ca,Na)(Si,Al) ₄ O ₈	Triclinic	51,00%
				Calcite	Ca(CO ₃)	Rhombohedral	3,10%
JH-43	White Building	-1,6568955	-78,6652079	Thenardite	Na ₂ SO ₄	Orthorhombic	34,00%
				Albite	(Na,Ca)Al(Si,Al) ₃ O ₈	Triclinic	66,00%
JH-44	White Building	-1,6583911	-78,664756	Thenardite	Na ₂ SO ₄	Orthorhombic	21,70%
				Anorthite	(Ca,Na)(Si,Al) ₄ O ₈	Triclinic	70,40%
				Calcite	Ca(CO ₃)	Rhombohedral	7,80%
JH-45	White Building	-1,6592087	-78,6654057	Thenardite	Na ₂ SO ₄	Orthorhombic	100%
JH-48	Gray Building	-1,650474	-78,6706452	Thenardite	Na ₂ SO ₄	Orthorhombic	60,60%
				Anorthite	(Ca,Na)(Si,Al) ₄ O ₈	Triclinic	32,50%
				Calcite	Ca(CO ₃)	Rhombohedral	6,90%
JH-50	White Building	-1,6519976	-78,6693208	Thenardite	Na ₂ SO ₄	Orthorhombic	45,90%
				Albite	(Na,Ca)Al(Si,Al) ₃ O ₈	Triclinic	21,50%
				Magnesium Calcite	(Mg _{0,03} , Ca _{0,97})(CO ₃)	Rhombohedral	32,70%
JH-51	White Building	-1,6522339	-78,6691366	Thenardite	Na ₂ SO ₄	Orthorhombic	76,30%
				Anorthite	(Ca,Na)(Si,Al) ₄ O ₈	Triclinic	23,70%
JH-53	White Building	-1,6535134	-78,6679597	Thenardite	Na ₂ SO ₄	Orthorhombic	46,30%
				Albite	(Na,Ca)Al(Si,Al) ₃ O ₈	Triclinic	38,60%
				Calcite	Ca(CO ₃)	Rhombohedral	15,10%
JH-57	White Building	-1,6562609	-78,6674157	Thenardite	Na ₂ SO ₄	Orthorhombic	59,20%
				Anorthite	(Ca,Na)(Si,Al) ₄ O ₈	Triclinic	36,30%
				Calcite	Ca(CO ₃)	Rhombohedral	4,50%
JH-58	White Building	-1,656476	-78,6670776	Thenardite	Na ₂ SO ₄	Orthorhombic	100%

Sample	Building Kind	Coordinates		Mineral Phase	Formula	Crystal System	%
		Latitude	Longitude				
JH-60	White Building	-1,6573056	-78,6660176	Thenardite	Na ₂ SO ₄	Orthorhombic	35,70%
				Anorthite	(Ca,Na)(Si,Al) ₄ O ₈	Triclinic	59,20%
				Calcite	Ca(CO ₃)	Rhombohedral	5,10%
JH-62	White Building	-1,658468	-78,6663918	Thenardite	Na ₂ SO ₄	Orthorhombic	73,10%
				Albite	(Na,Ca)Al(Si,Al) ₃ O ₈	Triclinic	22,10%
				Calcite	Ca(CO ₃)	Rhombohedral	4,80%
JH-67	White Building	-1,6489553	-78,6720739	Nitratine	NaNO ₃	Rhombohedral	100%

Sulfates:

The set of salts that are composed of: a cation joined with the anion SO_4 are known as sulfates. As is present in the results, the only one sulfate acting over the buildings in Riobamba city is thenardite. Thenardite (NaSO_4) corresponds to the stable anhydrous phase of the $\text{Na}_2\text{SO}_4\text{-H}_2\text{O}$ system. The other phase is Mirabilite ($\text{Na}_2\text{SO}_4\text{-10H}_2\text{O}$) which corresponds to the hydrated stable phase. Both phases are responsible for the deterioration of architectural structures. Thenardite precipitates directly from a solution when the temperature exceeds 32.4°C . The formation of mirabilite is dependent on temperature and relative humidity (RH) conditions. Mirabilite is stable between 20 to 32.4°C and RH above 71%. If the RH decreases mirabilite begins to turn into thenardite (Arnold & Zehnder, 1994). In addition, (Rodriguez-Navarro et al., 2000) demonstrate that under low RH or high evaporate rate conditions, thenardite precipitates directly from a solution at temperatures even less than 20°C .

Thenardite appears in thirty-one of the thirty-two samples analyzed. According to Zheng et al. (2010), thenardite is a typical sulfate formed in tropical to subtropical and equatorial sub-arid to arid zones. The damage produced by thenardite is associated with two processes. The first corresponds to the direct precipitation (crystallization) of thenardite inside the pores of mortars. The second process is the hydration of thenardite forming mirabilite. Both processes are capable to produce enough internal pressure over the pores to crack them, producing the deterioration of the mortar (Rodriguez-Navarro et al., 2000).

Carbonates:

Carbonates correspond to a set of salts formed by the combination of a cation with the carbonate (CO_3)²⁻ anion. The most common carbonates responsible for the deterioration of architectural structures around the world correspond to calcite, aragonite, and vaterite. In Riobamba city, the carbonates responsible of the deterioration process corresponds to calcite and magnesium calcite. Calcite $\text{Ca}(\text{CO}_3)$ is present in 22 of the 32 samples while. magnesium calcite is only present in two. Both carbonates represent 9% of the total amount of salts.

According to Dalton et al. (2022), the formation of calcite $\text{Ca}(\text{CO}_3)$ is a common problem in mortars around the world. In Portland mortars, calcite crystallized when calcium hydroxide ($\text{Ca}(\text{OH})_2$) reacts with CO_2 .

Calcium hydroxide (CH) is one of the major phases formed after the combination of Portland cement with water. The major amount of CH reacts and disappears during the process of cement setting. However, little quantities of CH could remain stored in pores posterior setting process (Bache et al., 1966). On the other hand, the main source of CO₂ corresponds to the atmosphere. The chemical reaction that forms calcite takes in place inside the pores located at the most superficial shell of mortars. This reaction occurs efficiently at RH conditions of 50 to 70% (Dalton et al., 2022).

The reaction that forms calcite begins with the infiltration of water inside the mortar. The water leaching the CH stored inside the pores forms a solution. Posteriorly, when this solution arrives at the most external shell in the mortar reacts with the CO₂ present in the atmosphere according to equation (1). Finally, calcite precipitates inside the pores (Šavija & Luković, 2016).



Magnesium calcite occurs when some magnesium atoms substitute the calcium atoms in the chemical structure of calcite. In both samples of magnesium calcite, the proportion of magnesium respects to calcium is 0,03Mg/0.97Ca.

The damage process associated with carbonates on mortars results from the nucleation of calcite inside the most external pores in the mortar. When calcite fill the pores, this exerts pressure over the internal walls of the pores. This pressure is enough to break the pores producing the efflorescence of the salts and leading a posterior alveolar erosion.

Nitrates:

Nitrates correspond to salts formed by a cation joined with the anion (NO₃)¹⁻. The only nitrate that involved in the deterioration process of architectural structures in Riobamba city corresponds to nitratine. Nitratine is present in only one sample of the 32 taken and represents the 100% of salt in the sample. This is interesting because the rest of the samples are composed of: two or three different salts (Table 6).

According to García-Florentino et al. (2016) and Ma et al. (2021), the formation of sodium nitrate or nitratine depends on the amount of nitrates and sodium present in the environment and the RH conditions.

Nitrates in general are solved in the atmosphere and water. While, sodium come from different sources because it is the sixth more abundant element in the earth (Ma et al., 2021). Nitratine Na (NO₃) crystallize efficiently on a RH between 20 to 30%.

Table 3 shows that the amount of Na₂O present in the R-DAD, from where sands and stones by buildings are mined, varies from 3.12 to 4.52 wt%. In addition, different studies about the water quality in the city reveal that the amount of nitrates solved varies from 1 to 3.7 mg/L (Muñoz, 2020). When water infiltrates in the mortars, this leaches the Na cations remnant from the sand previously employed. This cations reacts with the nitrates solved in the water to form Na(NO₃). Posteriorly Na(NO₃) solved in the water crystallizes inside the pores located at the most external shell of the mortar Marszałek et al. (2020). The internal pressure applied by the crystallization process eventually breaks the pores producing efflorescence. Under the action of winds efflorescence turns into alveolar erosion producing the deterioration of the mortar.

8 Discussion

The deterioration of architectural structures associated with physical weathering by salt growing has been a constant problem around the world. According to Hack (2020), Physical weathering is a natural phenomenon where groundmasses turn into small fragments by the action of forces but maintain the same chemical composition (Panchuk & Earle, 2015).

In Riobamba the deterioration of architectural structures associated with salt growing is a common problem present in the different neighborhoods of the city. From the architectural point of view, the different architectural structures in the city are classified in two groups: historical heritage buildings, and republican buildings (Lemache, 2017). In conformity with the observations, the deterioration process related to salt growing especially affects republican buildings. Even though, this phenomenon is also present in historical heritage private buildings. It is related to the zones that have been covered or fixed employing modern mortars. In addition, historical heritage public buildings (now when this study was done) were given maintenance due to, there was not found salts. In general, the degree of deterioration of buildings in Riobamba city is moderate. This is affirmed on the basis that the deterioration process only affects facades and walls. In other words, this only affects the aesthetics appearance of the house and does not represent a structural danger to it. In addition, the incidence of this phenomenon in the city is high because it is present in the city at any time of the year. It is important to clarify that these statements are made by the researcher based on the information collected and the results obtained.

The principal component in republican buildings corresponds to Portland cement, bricks (terracotta and concrete), iron rods, aggregates, and water. From these, only aggregates and water come from Riobamba. The aggregates are mined and expended by the quarries. The aggregates expended correspond to fine sand, medium to coarse sand and ripio. In addition, a few quarries also spend another kind of sand that consists of coarse sand obtained from the shredded process. Likewise, the water employed in the city comes from wells. The chemical analysis done about the water quality reveals the presence of sulfates and nitrates solved (Muñoz, 2020).

Aggregates, water and cement are the raw material by the different mortars and concrete. Fine sand mixed with cement and water form plaster mortars that will be employed in the endings of the buildings. In other words, this mortar is used to cover walls and concrete

columns. The mortar formed by the mix of medium to coarse sand with water and cement is employing to join the bricks to build walls. And finally, the concrete is the result of mixing ripio, medium to coarse sand, cement, and water. Concrete is employed to cover iron rods in columns and slabs. These are responsible for the structural stability of the building.

The observations carried through the city reveal that the deterioration process is principally related to mortars employed in the endings and in a few cases associated with mortars that joint bricks. Only in one case salt growing was associated with the deterioration of the concrete. However, this case takes in place in an abandoned property (Figure 15).

In addition, the presents study reveals that the principal mineral phases present in the process of the deterioration of architectural structures in Riobamba city, in order of abundance correspond to thenardite, albite, calcite, anorthite, magnesium calcite, and nitratine. From these minerals, albite, and anorthite corresponds to plagioclase remnant from the sand used in the mortar preparation, and they are not considered responsible for the deterioration process. By a better compression of the deterioration problem, the mineral phases are classified in salts according to their chemical composition. The different salts found in the architectural structures of the city correspond to: sulfates (thenardite), carbonates (calcite, magnesium calcite), and nitrates (nitratine) (Figure 24). Sulfates and carbonates are present in 31 of the 32 samples analyzed. Likewise, nitrates are only present in one sample however this sample is formed 100% by nitratine.

The sulfates correspond to salts forming in base to the sulfate (SO_4)²⁻ anion. Thenardite (Na_2SO_4) is a sulfate composed of: the cation Na^{1+} and the anion (SO_4)²⁻. According to Rodriguez-Navarro et al. (2000), thenardite precipitates direct from a solution when this exceeds a temperature of 32.4°C. Thenardite is the anhydride phase of the $\text{Na}_2\text{SO}_4\text{-H}_2\text{O}$ system, which is very soluble in water under temperature conditions of 0 to 32.38°C. (Bharmoria et al., 2014). According to the observations carried over the building materials employed in the architectural structures, sulfates are especially present in sieved sands and water.

According to Dalton et al. (2022), carbonates correspond to salts forming in base to the anion (CO_3)²⁻. The principal carbonates found in Riobamba corresponds to calcite $\text{Ca}(\text{CO}_3)$ and Magnesium calcite ($\text{Mg}_{0.03}, \text{Ca}_{0.97})(\text{CO}_3)$. Calcite crystallizes in Portland mortar when calcium hydroxide $\text{Ca}(\text{OH})_2$ reacts with CO_2 . This reaction occurs efficiently at RH conditions of 50

to 70% (Dalton et al., 2022). The main source of CO₂ is the atmosphere. On the other hand, calcium hydroxide, CH to abbreviate, is one of the major phases formed after the combination of Portland cement with water. The major amount of CH reacts and disappears during the process of cement setting. However, little quantities of CH could remain stored in pores posterior to the setting process (Bache et al., 1966). The reaction that describes the calcite formation is the following: $Ca(OH)^2 + CO_2 \rightarrow CaCO_3 + H_2O$. Magnesium calcite (Mg_{0,03}, Ca_{0,97})(CO₃) occurs when some magnesium atoms replace calcium atoms in the chemical structure of the calcite. The proportion of magnesium respects to calcium is 0,03Mg/0.97Ca (Šavija & Luković, 2016).

Finally, nitrates correspond to salts forming in base to the anion (NO₃)¹⁻. The main nitrate responsible for the deterioration process is nitratine. The formation of nitratine or sodium nitrate Na NO₃ depends on the RH conditions of 20 to 30%, and the amount of nitrates and sodium present in the environment (García-Florentino et al., 2016; Ye, 2021). In Riobamba city the main source of nitrates is the water employed by the citizens (Muñoz, 2020). Likewise, the source of Na corresponds to sands employed to prepare the mortar. According to Marszałek et al. (2020), Na NO₃ solved in the water crystallizes inside the pores located at the most external shell of the mortar.

From the exposure previously, the nucleation of each kind of salt is related to temperature and RH conditions. The temperature affects the solubility of many salts. Changes in the solubility properties affects the mobility of the salt within the water. This may produce that a salt precipitate in a pore, or on the other hand, the salt placed in a pore was leaching by the water. According to Ilbay-Yupa et al. (2021) and INAMHI (2017), the average temperature in Riobamba varies from 8 to 19 °C, though, in many cases the maximum temperature can arrives until the 22 °C. Likewise, the RH varies from 68 to 77%. Based on this, the temperature is not enough by the nucleation of thenardite, due to this salt is formed over the 32.4°C. However according to Torraca (2005), it is possible because the temperature inside the pores, where the salts precipitate, is higher than the average temperature of the environment.

9 Conclusion and Recommendation

9.1 Conclusion

The present study shows that deterioration in architectural structures by the action of salt growing is a recurrent problem in the city. Riobamba city from the architectural point of view it is constituted by two kinds of structures. The historical heritage buildings that correspond to 435 buildings located specially in the historical heritage center of the city, and the republican buildings which represents the principal kind of buildings with 30 819 structures distributed around the city. The deterioration process in historical heritage private buildings is limited to the zones that were covered or fixed with modern mortars as is shown in Figure 13. On the other hand, historical heritage public buildings were given maintenance, and did not find salts in these buildings.

Republican buildings consist in structures built in base of cement, bricks, iron rods, and aggregates. From the civil engineering point of view, republican buildings are classified according to the final construction state in white, gray, and black works buildings. The results show that, this phenomenon attacks specially to plaster mortars. The deterioration associated with salt growing manifest itself in the form of salt cumulus or efflorescence. After, efflorescence turns into alveolar erosion by the action of wind.

Efflorescence and alveolar erosion represent an aesthetic problem for the city because both associate the buildings with a deteriorated and careless aspect. This aesthetic problem turns into an economic problem when the listing value of the property decreases due to bad appearance, or when the house owners are forced to spend money periodically to maintain the good aspect of their homes.

The mineral phases involved in the deterioration process were determined from the XRD analysis of samples taken in the zone known as El Retamal. In this zone a total of 72 samples of efflorescence were taken from buildings. From these, only 32 were selected by the XRD analysis because it is considered representative enough of the total. The results show that the principal mineral phases associated in the deterioration process of architectural structures in Riobamba city ordered according to their abundance corresponds to: thenardite (Na_2SO_4), calcite (Ca CO_3), magnesium calcite ($\text{Mg}_{0,03}, \text{Ca}_{0,97}$)(CO_3), and nitratine (Na NO_3).

By a better understanding these mineral phases are classified in salts. The salts found as responsible for the deterioration of architectural structures in the city corresponds to: sulfates (thenardite), carbonates (calcite, magnesium calcite), and nitrates (nitratine). The crystallization of each salt depends of the temperature and RH conditions.

From these salts, sulfates are the most common salts evolved in the deterioration process. Thenardite (Na_2SO_4) corresponds at only one sulfate present in the samples. Thenardite is present in 31 of 32 samples taken in El Retamal. This salt and corresponds to the stable anhydrous phase of the $\text{Na}_2\text{SO}_4\text{-H}_2\text{O}$ system. The other phase is Mirabilite ($\text{Na}_2\text{SO}_4\cdot 10\text{H}_2\text{O}$) which corresponds to the hydrated stable phase. The damage produces by thenardite is associated at two processes. The first corresponds to the direct precipitation (crystallization) of thenardite inside the pores of mortars. The second process is the hydration of thenardite forming mirabilite. The nucleation of each kind of sulfates depends on temperature and RH conditions.

Carbonates represent the second set of salts involved in the deterioration process. The carbonates present corresponds to calcite and magnesium calcite. Calcite Ca CO_3 crystallizes in Portland mortar when calcium hydroxide Ca (OH)_2 reacts with CO_2 . Finally, the last group of salts involved corresponds to nitrates. From nitrates, the only one mineral phase present corresponds to nitratine. Nitratine Na NO_3 crystallize efficiently in a RH between 20 to 30% and his formation is limited by the amount of nitrates and sodium present in the environment.

These three groups of salts crystallize directly from a solution inside pores located at the most external shell of mortars, where the temperature and RH conditions are the right ones. In Riobamba the average temperature varies from 8° to 19°C though, in many cases the maximum temperature can arrive until the 22°C . This temperature is below that required by the nucleation of thenardite. However, it is possible because the temperature in the pores is higher than in the environment (Torraca, 2005).

The nucleation process realizes internal pressure over the pore walls. This pressure is responsible to break the pores producing the efflorescence of the salts. Posteriorly, efflorescence is affected by winds producing alveolar erosion. Alveolar erosion is the responsible for the disintegration of mortars.

From the exposure previously, the crystallization of salts is related to RH and temperature conditions, likewise, this also depends on sources that provide the anions and cations. The chemical reactions that form the salts occurs in water. Water penetrates and scrolls inside the mortars by diffusion and capillarity. Both processes employ pores and fissures as conducts for the water. When the water moves inside mortar, this leaches mortars assimilating anions, cations even salts, forming a solution. Posteriorly according to temperature and RH conditions, the different phase minerals crystallize from the solution placing inside the pores and fissures (Torraca, 2005).

The results from the chemical composition analyses of building materials reveal that the main source of salts, anions, and cations corresponds to aggregates. The aggregates are mined from the Riobamba Unit. For this reason, the aggregates correspond to volcano sedimentary material that supplies with anions and cations by the posterior formation of salts. Likewise, according with the results aggregates in addition with water are the largest supplier of sulfates. The chemical analyses carried over the aggregates reveal that Sulphur is mainly present in sieved fine sands. This sand is only employed by plaster mortars to cover walls columns and sometime roofs. This could explain why the deterioration process principally affects this kind of mortars due to the high sulfate concentration in this kind of aggregate. Likewise, this explain why salt growing deterioration is not common in mortar to join bricks and concretes.

In addition, the bibliography indicates other important sources of anions and cations. These correspond to the atmosphere and the hydrosphere. The present study prioritizes aggregates and water as the main sources responsible for the deterioration process. The chemical analyses carried over the aggregates reveal that Sulphur is only present in sieved fine sands. This could explain why the deterioration process principally affects the aesthetic aspect of the buildings, due to this sand is used in mortars employed in the endings covering walls, columns and sometimes roofs.

In complement, the nucleation the rest of salts (nitrates) could be attributed at the water quality employed in the city. The different studies over the water quality in Riobamba city reveals the presence of sulfates and nitrates solved in. In addition, the enunciated previously justify why the nucleation of salts in mortars employed to join bricks occurs. In this case, the main source of sulfate is water because Sulphur is missing in shredded medium to coarse sand.

9.2 Recommendations

In concordance with what was exposed in this project, the crystallization of each kind of salts related to RH and temperature conditions. Which affects the solubility and mobility of the salts solved in water. Likewise, this also depends on sources that provide the anions and cations. According to what was exposed in the discussion, the city provides adequate conditions for the precipitation of sulfates and carbonates. However, there is an inconsistency in the RH conditions for the nucleation of Nitrate NaNO_3 . This is because this salt needs RH conditions of 20 to 30%, but the RH in Riobamba varies from 68 to 77%. The present project recommends the study of any possible variation between the RH in the environment respect with to RH inside the pore. This could help to justify the presence of nitrate.

In addition, the amount of nitrates solved in the water is very low and there is the possibility of the existence of other nitrates sources. According to the bibliography, between the most important sources of nitrates are the fertilizers and the excreta from the animals. The fertilizers infiltrate the soil and contaminate the groundwater providing various chemical compounds including nitrates. Likewise, the excreta from animals especially the urine contains high concentrations of nitrates solved. These nitrates come into contact with the mortars when people and stray animals urinate or defecate on the walls. It is recommendable to analyse these factors to clarify the correct precedence of the nitrate in the deterioration process.

10 References

- Abdulrazzak, F. H., & Alkiam, A. F. (2019). *Behavior of X-Ray Analysis of Carbon Nanotubes*. 1–16.
- Adelca. (2020). *adelca EL ACERO QUE NOS UNE, CATALOGO DE PRODUCTOS*.
- Arnold, A., & Zehnder, K. (1994). *La conservazione dei monumenti nel bacino del Mediterraneo. October*.
- Bache, H. H., Idorn, G. M., Nepper-Christensen, P., & Nielsen, J. (1966). Morphology of Calcium Hydroxide in Cement Paste. *Symposium on Structure of Portland Cement Paste and Concrete*, 90, 154–174. <http://onlinepubs.trb.org/Onlinepubs/sr/sr90/90-014.pdf>
- Barba, D. (2016). Estudio Vulcanológico del Complejo Volcánico Chimborazo. *Escuela Politécnica Nacional*, 1–217. <http://bibdigital.epn.edu.ec/handle/15000/144>
- Barba, D., Robin, C., Samaniego, P., & Eissen, J. P. (2008). Holocene recurrent explosive activity at Chimborazo volcano (Ecuador). *Journal of Volcanology and Geothermal Research*, 176(1), 27–35. <https://doi.org/10.1016/j.jvolgeores.2008.05.004>
- Bernard, B., van Wyk de Vries, B., Barba, D., Leyrit, H., Robin, C., Alcaraz, S., & Samaniego, P. (2008). The Chimborazo sector collapse and debris avalanche: Deposit characteristics as evidence of emplacement mechanisms. *Journal of Volcanology and Geothermal Research*, 176(1), 36–43. <https://doi.org/10.1016/j.jvolgeores.2008.03.012>
- Bharmoria, P., Gehlot, P. S., Gupta, H., & Kumar, A. (2014). Temperature-dependent solubility transition of Na₂SO₄ in water and the effect of NaCl therein: Solution structures and salt water dynamics. *Journal of Physical Chemistry B*, 118(44), 12734–12742. <https://doi.org/10.1021/jp507949h>
- Buenaño, A. (2018). *Análisis geológico y geofísico aplicado a la prospección hidrogeológica entre las localidades de Riobamba y Pungalá*. 1–111.
- Chiaradia, M., Müntener, O., Beate, B., & Fontignie, D. (2009). Adakite-like volcanism of Ecuador: Lower crust magmatic evolution and recycling. *Contributions to Mineralogy and Petrology*, 158(5), 563–588. <https://doi.org/10.1007/s00410-009-0397-2>

- Clapperton, C. M. (1990). Glacial and volcanic geomorphology of the Chimborazo-Carihuairazo Massif, Ecuadorian Andes. *Transactions of the Royal Society of Edinburgh: Earth Sciences*, 81(2), 91–116. <https://doi.org/10.1017/S0263593300005174>
- Cobos, N., Romero, C. W., Dvořáková, K. V, Oñate, L., Condoy, D. P., Carranco, F. R., Castillo, M., Freyle, H., & Gramal, A. B. (2022). *Análisis de proveniencia de la unidad yaruquies, riobamba-ecuador* (Issue November). <https://doi.org/10.13140/RG.2.2.31501.00484>
- Dalton, L. E., Crandall, D., & Pour-Ghaz, M. (2022). Supercritical, liquid, and gas CO₂ reactive transport and carbonate formation in portland cement mortar. *International Journal of Greenhouse Gas Control*, 116, 0–2. <https://doi.org/10.1016/j.ijggc.2022.103632>
- Doehne, E. (2002). Salt Weathering: A Selective Review. *Geological Society Special Publication*, 205(Flatt), 51–64.
- García-Florentino, C., Maguregui, M., Morillas, H., Balziskueta, U., Azcarate, A., Arana, G., & Madariaga, J. M. (2016). Portable and Raman imaging usefulness to detect decaying on mortars from Punta Begoña Galleries (Getxo, North of Spain). *Journal of Raman Spectroscopy*, 47(12), 1458–1466. <https://doi.org/10.1002/jrs.4949>
- Gavilanes, C., & Santellan, G. (2016). “NORMALIZACIÓN Y ESTANDARIZACIÓN DE LA FABRICACIÓN DE LADRILLOS Y TEJAS DEL CANTÓN CHAMBO.”
- Hack, H. R. G. K. (2020). Weathering, Erosion, and Susceptibility to Weathering. *Soft Rock Mechanics and Engineering*, January, 291–333. https://doi.org/10.1007/978-3-030-29477-9_11
- Haynes, H. (2002). Sulfate Attack on Concrete: Laboratory vs. Field Experience. *Concrete International*, 24(7), 64–70.
- Haynes, H., O’Neill, R., & Mehta, P. K. (1996). Concrete deterioration from physical attack by salts. *Concrete International*, 18(1), 63–69.
- Ilbay-Yupa, M., Lavado-Casimiro, W., Rau, P., Zubieta, R., & Castellón, F. (2021). Updating regionalization of precipitation in Ecuador. *Theoretical and Applied Climatology*, 143(3–

- 4), 1513–1528. <https://doi.org/10.1007/s00704-020-03476-x>
- INAMHI. (2017). Anuario meteorológico № 53-2013. In J. Olmedo Moran (Ed.), *Instituto Nacional de Meteorología e Hidrología* (Issue 52). http://www.serviciometeorologico.gob.ec/docum_institucion/anuarios/meteorologicos/Am_2013.pdf
- Lemache, C. (2017). Filatelia postal de la iconografía arquitectónica neoclásica de Riobamba. In *UNIVERSIDAD NACIONAL DE CHIMBORAZO*. [http://dspace.unach.edu.ec/bitstream/51000/8192/3/Lara A.%3B Wilson %282021%29 Diseño e implementación de un sistema de agricultura de precisión%2C para la optimización del agua de riego del Cantón Chambo..pdf](http://dspace.unach.edu.ec/bitstream/51000/8192/3/Lara_A.%3B_Wilson_%282021%29_Diseño_e_implementación_de_un_sistema_de_agricultura_de_precisión%2C_para_la_optimización_del_agua_de_riego_del_Cantón_Chambo..pdf)
- Ma, S., Pang, S., Li, J., & Zhang, Y. (2021). A review of efflorescence kinetics studies on atmospherically relevant particles. *Chemosphere*, 277, 130320. <https://doi.org/10.1016/j.chemosphere.2021.130320>
- MAGAP. (2012). *Memoria Técnica Cantón Guano Proyecto: “ Generación de Geoinformación para la gestión del territorio a nivel nacional escala 1:25.000”*. 64. <https://outlook.live.com/owa/?mkt=es-us&path=/attachmentlightbox>
- Mancheno, N. P. (2010). *Análisis de la problemática y ampliación del sistema de agua potable en la ciudad de Riobamba*. 126. https://repositorio.espe.edu.ec/bitstream/21000/1685/2/T-ESPE-027486.pdf?fbclid=IwAR36X7br4CK5JLMKzJjd_xYNJcsvWu2WqAWei_b14cFKvFd4bmak6Xks0Kk
- Marszałek, M., Dudek, K., & Gawel, A. (2020). Cement render and mortar and their damages due to salt crystallization in the holy trinity church, dominicans monastery in cracow, poland. *Minerals*, 10(7), 1–19. <https://doi.org/10.3390/min10070641>
- Muñoz, G. P. (2020). *Evaluación de la calidad del agua subterránea de Riobamba mediante el índice de calidad de agua ICA-NSF*. 14. <https://all3dp.com/2/fused-deposition-modeling-fdm-3d-printing-simply-explained/>
- Noblet, C., Dugas, F., & Vera, R. (1990). *Sedimentación continental en las cuencas intramontañosas terciarias del Ecuador*. 141–150.

- NTE INEN 2380. (2011). Requisitos de desempeño para cementos hidráulicos: NTE-INEN-2380. *Inen*, 1(Primera Edición), 5. <http://181.112.149.203/buzon/normas/2380.pdf>
- Orna, J. (2019). “IMPLEMENTACION DE UN PROCEDIMIENTO QUE ESTIME RESISTENCIAS A COMPRESIÓN EN PASTA DE CEMENTO POR TERMOMETRÍA, EN LA EMPRESA UNIÓN CEMENTERA NACIONAL UCEM S.A –PLANTA CHIMBORAZO” TRABAJO.
- Palma-Henríquez, J. (2018). Las regiones naturales. *Unae*, 351–471. <http://repositorio.unae.edu.ec/bitstream/56000/944/1/TFM-EGH-38.pdf>
- Panchuk, K., & Earle, S. (2015). Chapter 8 . Weathering , Sediment , & Soil. In *Physical Geology, First University of Saskatchewan Edition* (pp. 1–25).
- Pourrut, P. (1983). *LOS CLIMAS DEL ECUADOR . FUNDAMENTOS EXPLICATIVOS Pierre POURRUT Hidrólogo de la ORSTOM Apartado 6596 CCI - QUITO.* https://horizon.documentation.ird.fr/exl-doc/pleins_textes/divers11-10/21848.pdf
- Price. (1995). Weathering and weathering processes. *Quarterly Journal of Engineering Geology*, 28(3), 243–252. <https://doi.org/10.1144/gsl.qjegh.1995.028.p3.03>
- Price, C. (2000). *An Expert Chemical Model for Determining the Environmental Conditions Needed to Prevent Salt Damage in Porous Materials.*
- Rodriguez-Navarro, C., Doehne, E., & Sebastian, E. (2000). How does sodium sulfate crystallize? Implications for the decay and testing of building materials. *Cement and Concrete Research*, 30(10), 1527–1534. [https://doi.org/10.1016/S0008-8846\(00\)00381-1](https://doi.org/10.1016/S0008-8846(00)00381-1)
- Romero, W., & Chuquimarca, C. (2011). “ESTUDIO DEL PROCESO DE FABRICACIÓN PARA OBTENER BLOQUES HUECOS DE HORMIGÓN PARA MAMPOSTERÍA CON RESISTENCIA A LA COMPRESIÓN DE 2,5 Y 4 MPa EN LA CIUDAD DE RIOBAMBA.”
- Ruiz, G. M. H., Seward, D., & Winkler, W. (2007). Chapter 36 Evolution of the Amazon Basin in Ecuador with Special Reference to Hinterland Tectonics: Data from Zircon Fission-Track and Heavy Mineral Analysis. In *Developments in Sedimentology* (Vol. 58, Issue 07, pp. 907–934). [https://doi.org/10.1016/S0070-4571\(07\)58036-2](https://doi.org/10.1016/S0070-4571(07)58036-2)
- Salguero, D. A. (2017). Levantamiento geológico-estructural de la zona comprendida por la

Hoja Topográfica de Guano Escala 1: 50000, Provincia de Chimborazo. *Escuela Politécnica Nacional. Proyecto de Titulación. Quito, Ecuador.*, 244.

Samaniego, P., Barba, D., Robin, C., Fornari, M., & Bernard, B. (2012). Eruptive history of Chimborazo volcano (Ecuador): A large, ice-capped and hazardous compound volcano in the Northern Andes. *Journal of Volcanology and Geothermal Research*, 221–222, 33–51. <https://doi.org/10.1016/j.jvolgeores.2012.01.014>

Šavija, B., & Luković, M. (2016). Carbonation of cement paste: Understanding, challenges, and opportunities. *Construction and Building Materials*, 117, 285–301. <https://doi.org/10.1016/j.conbuildmat.2016.04.138>

Tapia, F. (2015). VULNERABILIDAD DE LOS HORMIGONES MASIVOS FRENTE AL FENÓMENO EXPANSIVO POR FORMACIÓN DE ETRINGITA TARDÍA, EN FUNCIÓN DEL CONTENIDO DE PUZOLANA EN CEMENTOS NACIONALES. In *Metrologia* (Vol. 53, Issue 5). http://publicacoes.cardiol.br/portal/ijcs/portugues/2018/v3103/pdf/3103009.pdf%0Ahttp://www.scielo.org.co/scielo.php?script=sci_arttext&pid=S0121-75772018000200067&lng=en&tlng=en&SID=5BQIj3a2MLaWUV4OizE%0Ahttp://scielo.iec.pa.gov.br/scielo.php?script=sci_

Torraca, G. (2005). *POROUS BUILDING MATERIALS Materials Science for Architectural Conservation*. ICCROM.

Val, A. L., De Almeida-Val, V. M. F., & Randall, D. J. (2005). Tropical Environment. In *Fish Physiology* (Vol. 21, Issue C, pp. 1–45). [https://doi.org/10.1016/S1546-5098\(05\)21001-4](https://doi.org/10.1016/S1546-5098(05)21001-4)

Vallejo, C., Spikings, R. A., Luzieux, L., Winkler, W., Chew, D., & Page, L. (2006). The early interaction between the Caribbean Plateau and the NW South American Plate. *Terra Nova*, 18(4), 264–269. <https://doi.org/10.1111/j.1365-3121.2006.00688.x>

Vallejo Cruz, C. (2007). Evolution of the Western Cordillera in the Andes of Ecuador (Late Cretaceous-Palogen). *SWISS FEDERAL INSTITUTE OF TECHNOLOGY ZÜRICH*, 17023.

Vecco, M. (2010). A definition of cultural heritage: From the tangible to the intangible. *Journal of Cultural Heritage*, 11(3), 321–325.

<https://doi.org/10.1016/j.culher.2010.01.006>

Winkler, W., Villagómez, D., Spikings, R., Abegglen, P., Tobler, S., & Egüez, A. (2005). The Chota basin and its significance for the inception and tectonic setting of the inter-Andean depression in Ecuador. *Journal of South American Earth Sciences*, 19(1 SPEC. ISS.), 5–19. <https://doi.org/10.1016/j.jsames.2004.06.006>

Ye, H. (2021). Autogenous formation and smart behaviors of nitrite- and nitrate-intercalated layered double hydroxides (LDHs) in Portland cement-metakaolin-dolomite blends. *Cement and Concrete Research*, 139(October 2020), 106267. <https://doi.org/10.1016/j.cemconres.2020.106267>

Zheng, M., Zhao, Y., & Liu, J. (2010). Palaeoclimatic Indicators of China's Quaternary Saline Lake Sediments and Hydrochemistry. *Acta Geologica Sinica - English Edition*, 74(2), 259–265. <https://doi.org/10.1111/j.1755-6724.2000.tb00459.x>

11 Annexes

Annex 1. Table of chemical characteristics of water from the different wells that supplies to Riobamba city.

	Sulfates (mg/L)	Nitrates (mg/L)	PH
Vertiente San Pablo	14	2	6,89
Pozo Llío 1	9	1	7,13
Pozo Llío 2	9	1,1	6,58
Pozo Llío 3	10	1,7	7,12
Pozo Llío 4	12	1,7	6,7
Pozo Llío 5	9	1,6	6,52
Pozo Llío 6	4	1,2	6,6
Pozo Llío 7	8	2	6,7
Pozo 24 de mayo	430	2,3	7,1
Pozo Huerta	60	1,7	7,38
Pozo Servidores	70	1,1	7,44
Pozo Hierbas	96	1,9	7,22
Pozo 21 de abril	200	1,9	7,63
Pozo San Gabrie	98	2	7,39
Pozo Las Abras	210	3,7	7,65
Pozo Maldonado	14	1,7	7,76
Pozo Lascano	480	2,1	7,89
Pozo El Estadio	105	3,4	7,75

Annex 2. Table of aggregates expended in each quarry active in Riobamba city.

Quarry	Material					
	Sieve sand		Sieve ripio	Shredded sand		Shredded ripio
	Fine	Medium to Coarse		Fine	Medium to Coarse	
Cerro Negro	X	X	X	-	X	X
El cisne	X	X	X	-	-	-
Mira Flores	X	X	X	-	-	-
La Ponderosa	X	X	X	-	-	-
Sillahuan	X	X	X	-	X	X

Annex 3. Table of hand sample description of the different rocks that constitute the Ripio expanded in the different quarries in Riobamba city.

PETROGRAPHIC DESCRIPTION	
Component Features	
Color	Light gray
Texture	Porphyritic
Structure	Massive
Crystal Size	1-2 mm
Crystal shape	Euhedral to subhedral
% Phenocrysts:	25
% Matrix:	75
Mineral Content	
Main Minerals	Amphibole, pyroxene, plagioclase.
Secondary Minerals	-
Minerals Accessories	-
Mineralization	-
Degree of weathering	Low
Type of alteration	-
Rock's name	Amphibole andesites



PETROGRAPHIC DESCRIPTION	
Component Features	
Color	Brow
Texture	Porphyritic
Structure	Massive
Crystal Size	1 mm
Crystal shape	Euhedral to subhedral
% Phenocrysts:	40
% Matrix:	60
Mineral Content	
Main Minerals	Amphibole, pyroxene, plagioclase.
Secondary Minerals	-
Minerals Accessories	Quartz
Mineralization	-
Degree of weathering	Low
Type of alteration	-
Rock's name	Amphibole-pyroxene andesites



PETROGRAPHIC DESCRIPTION	
Component Features	
Color	Reddish
Texture	Porphyritic
Structure	Massive
Crystal Size	1 mm
Crystal shape	Euhedral to subhedral
% Phenocrysts:	15
% Matrix:	80
Mineral Content	
Main Minerals	Pyroxene, amphibole, plagioclase.
Secondary Minerals	-
Minerals Accessories	Quartz
Mineralization	-
Degree of weathering	Low
Type of alteration	-
Rock's name	Amphibole-plagioclase andesites



PETROGRAPHIC DESCRIPTION	
Component Features	
Color	Gray
Texture	Porphyritic
Structure	Massive
Crystal Size	1-3 mm
Crystal shape	Euhedral to subhedral
% Phenocrysts:	45
% Matrix:	55
Mineral Content	
Main Minerals	Pyroxene, amphibole, plagioclase.
Secondary Minerals	-
Minerals Accessories	Quartz
Mineralization	-
Degree of weathering	Low
Type of alteration	-
Rock's name	Andesite



Annex 4. Table of samples taken in EL Retamal. The table indicates the specific location of each sample from where was taken, likewise, specifies the kind of building and the walling material where the salt is affecting.

Sample	Latitude	Longitude	Structure	Kind of Building	Walling Material
JH-01	9817517,873	758950,2282	Closing brick wall	Gray work buildings	Mortar for bricks
JH-02	9817463,039	758939,4215	Home facade	White work buildings	Plaster mortar
JH-03	9817338,888	759023,7358	Home facade	White work buildings	Plaster mortar
JH-04	9817323,51	759033,9482	Home facade	White work buildings	Plaster mortar
JH-05	9817302,087	759048,7734	Home facade	White work buildings	Plaster mortar
JH-06	9817286,38	759057,2377	Home facade	Gray work buildings	Plaster mortar
JH-07	9817261,256	759087,1426	Closing brick wall	Black work buildings	Mortar for bricks
JH-08	9817227,306	759105,2483	Home facade	Gray work buildings	Plaster mortar
JH-09	9817211,153	759116,4505	Home facade	Gray work buildings	Plaster mortar
JH-10	9817194,116	759136,5352	Closing brick wall	Black work buildings	Mortar for bricks
JH-11	9817174,679	759137,0356	Home facade	Gray work buildings	Plaster mortar
JH-12	9817076,364	759206,7189	Home facade	White work buildings	Plaster mortar
JH-13	9817077,607	759203,3918	Home facade	White work buildings	Plaster mortar
JH-14	9817056,443	759223,4828	Home facade	White work buildings	Plaster mortar
JH-15	9817005,764	759226,0059	Home facade	White work buildings	Plaster mortar
JH-16	9816835,146	759275,9335	Home facade	White work buildings	Plaster mortar
JH-17	9816838,267	759312,2725	Home facade	White work buildings	Plaster mortar
JH-18	9816757,152	759346,3639	Home facade	White work buildings	Plaster mortar
JH-19	9816756,873	759347,7885	Home facade	White work buildings	Plaster mortar
JH-20	9816682,488	759368,2509	Home facade	White work buildings	Plaster mortar
JH-21	9816631,44	759421,4915	Home facade	White work buildings	Plaster mortar
JH-22	9816747,994	759137,7591	Home facade	White work buildings	Plaster mortar
JH-23	9816747,994	759137,7591	Home facade	White work buildings	Plaster mortar
JH-24	9816459,369	759614,9325	Home facade	White work buildings	Plaster mortar
JH-25	9816463,531	759631,6356	Home facade	White work buildings	Plaster mortar
JH-26	9816423,328	759671,0628	Home facade	White work buildings	Plaster mortar
JH-27	9817541,481	759005,8944	Home facade	White work buildings	Plaster mortar
JH-28	9817503,1	759020,8445	Home facade	White work buildings	Plaster mortar
JH-29	9817425,701	759026,8543	Home facade	Gray work buildings	Plaster mortar
JH-30	9817404,624	759086,1752	Home facade	White work buildings	Plaster mortar
JH-31	9817366,684	759111,3339	Home facade	White work buildings	Plaster mortar
JH-32	9817221	759247,7103	Home facade	White work buildings	Plaster mortar
JH-33	9817182,15	759265,5763	Home facade	White work buildings	Plaster mortar
JH-34	9817096,21	759329,0512	Home facade	White work buildings	Plaster mortar
JH-35	9817029,771	759384,3891	Home facade	White work buildings	Plaster mortar
JH-36	9816974,173	759458,297	Home facade	White work buildings	Plaster mortar

JH-37	9816930,701	759502,7857	Home facade	White work buildings	Plaster mortar
JH-38	9816890,598	759552,132	Home facade	White work buildings	Plaster mortar
JH-39	9816866,189	759575,5253	Home facade	White work buildings	Plaster mortar
JH-40	9816839,101	759600,3293	Closing brick wall	Black work buildings	Terracotta brick
JH-41	9816831,095	759616,5172	Home facade	White work buildings	Plaster mortar
JH-42	9816805,451	759646,0318	Home facade	White work buildings	Plaster mortar
JH-43	9816709,651	759768,2727	Home facade	White work buildings	Plaster mortar
JH-44	9816544,143	759818,3838	Home facade	White work buildings	Plaster mortar
JH-45	9816453,783	759745,9514	Home facade	White work buildings	Plaster mortar
JH-46	9817518,123	759105,1103	Home facade	Gray work buildings	Plaster mortar
JH-47	9817446,576	759149,2769	Home facade	White work buildings	Plaster mortar
JH-48	9817420,728	759163,8186	Closing brick wall	Black work buildings	Concrete brick
JH-49	9817311,608	759268,912	Home facade	White work buildings	Plaster mortar
JH-50	9817252,01	759311,0553	Home facade	White work buildings	Plaster mortar
JH-51	9817225,846	759331,5301	Home facade	White work buildings	Plaster mortar
JH-52	9817192,826	759321,439	Home facade	White work buildings	Plaster mortar
JH-53	9817084,15	759462,3782	Home facade	White work buildings	Plaster mortar
JH-54	9817068,74	759480,9842	Home facade	Gray work buildings	Plaster mortar
JH-55	9816966,27	759574,8639	Home facade	White work buildings	Plaster mortar
JH-56	9816851,736	759570,9775	Home facade	White work buildings	Plaster mortar
JH-57	9816780,142	759522,5796	Home facade	White work buildings	Plaster mortar
JH-58	9816756,303	759560,1894	Home facade	White work buildings	Plaster mortar
JH-59	9816694,027	759630,5604	Home facade	White work buildings	Plaster mortar
JH-60	9816664,391	759678,0821	Home facade	White work buildings	Plaster mortar
JH-61	9816529,81	759693,5975	Home facade	White work buildings	Plaster mortar
JH-62	9816535,851	759636,274	Home facade	White work buildings	Plaster mortar
JH-63	9817588,917	759004,9702	Home facade	White work buildings	Plaster mortar
JH-64	9817943,966	758756,3199	Home facade	White work buildings	Plaster mortar
JH-65	9818473,52	758412,0063	Home facade	Gray work buildings	Plaster mortar
JH-66	9819003,073	758067,6926	Home facade	White work buildings	Plaster mortar
JH-67	9817532,627	757723,379	Home facade	White work buildings	Plaster mortar
JH-68	9817395,514	757379,0653	Home facade	Gray work buildings	Plaster mortar
JH-69	9816925,067	757034,7517	Home facade	Gray work buildings	Plaster mortar
JH-70	9816676,843	756690,438	Home facade	White work buildings	Plaster mortar
JH-71	9817373,063	756346,1244	Home facade	White work buildings	Plaster mortar
JH-72	9817069,283	756001,8107	Home facade	White work buildings	Plaster mortar